GEOPHYSICAL DELINEATION AND MONITORING OF AMD IN THE CRADLE OF HUMANKIND

Report to the

Water Research Commission

by

Michael van Schoor

CSIR

WRC Report No 2440/1/18

ISBN 978-0-6392-0041-5

October 2018

Obtainable from:

Water Research Commission
Private Bag X03
Gezina, 0031

orders@wrc.org.za or download from www.wrc.org.za

Printed in the Republic of South Africa

TABLE OF CONTENTS

LIST OF FIGURES

LIST OF TABLES

ABBREVIATIONS

AMD	Acid Mine Drainage
COH	Cradle of Humankind
DWS	Department of Water and Sanitation
ERT	Electrical Resistance Tomography
KGR	Krugersdorp Game Reserve
WRC	Water Research Commission

1 INTRODUCTION

This report summarises the findings of Project K5/2440: *Geophysical delineation and monitoring of acid mine drainage (AMD) in the Cradle of Humankind (COH)*. This was a two-year project. For this reason, this report focuses primarily on the Year 2 deliverables (Deliverable 4 and Deliverable 5 in Table 1); however, for the sake of completeness, a full project overview/background summary is also included here to address all Year 1 and Year 2 aims and associated deliverables.

Table 1: Summary of project aims and associated activities/deliverables

Aim/deliverable number	Description
1	**Activity 1: Spectral complex resistivity property analysis** Representative rock and groundwater samples from the study area will be analysed at laboratory scale to determine the relationships between the relevant geophysical and physiochemical properties.
2	**Activity 2: Numerical and physical scale model studies** Synthetic geoelectric models that represent realistic/anticipated field scenarios will be used in a series of model studies aimed at establishing the optimum field survey parameters and to predict the performance of the geophysical methods.
3	**Activity 3: Two-dimensional electrical resistance tomography (ERT) field measurements** Two-dimensional ERT survey results from strategically selected locations around the perimeter of the inferred AMD pseudo-plume will contribute to an improved understanding of the lateral extent of the AMD footprint.
4	**Activity 4: Follow-up ERT field measurements and implementation of dynamic monitoring** Repeat surveys after a year and comparison of the results with the initial baseline surveys are aimed at highlighting transient changes in geophysical field parameters that may reflect changes in the shape, extent and/or intensity of the AMD footprint. The subsequent and ultimate project aim is to define an ongoing monitoring methodology for future use.
5	Definition of a geophysical monitoring methodology /strategy that can be applied on an ongoing basis, if required.

The main aim of the project was to assess the applicability of the time-lapse ERT survey method to monitor changes in local aquifer contamination levels (sulphate content). The extent of the study area is depicted in Figure 1, which also provides some useful background information and the rationale behind this project.

Figure 1 shows the AMD footprint as postulated by Hobbs (2013) on the basis of geohydrological field observations. For this project (K5/2440), geophysical test sites were selected around the perimeter of the inferred AMD footprint that covered a range of pollution scenarios – ranging from highly polluted to virtually contaminant-free. The objective of K5/2440 comprised:

- Characterising and quantifying the electrical resistivity of the dolomitic aquifer and consequently establishing baseline geophysical snapshots for these test sites (Year 1).
- Revisiting these sites after approximately 12 months and repeating the resistivity surveys.

Transient changes in the groundwater quality, in particular the sulphate concentration, were expected to manifest as corresponding changes in baseline resistivity responses. If these changes in resistivity responses could be reliably correlated with the changes in water quality, it would indicate that time-lapse resistivity surveys could be employed to supplement the ongoing borehole-based groundwater monitoring programme. Ongoing geophysical monitoring efforts could help to improve the lateral

accuracy of the AMD footprint delineation, obviating the need to add significantly to the existing network of monitoring boreholes.

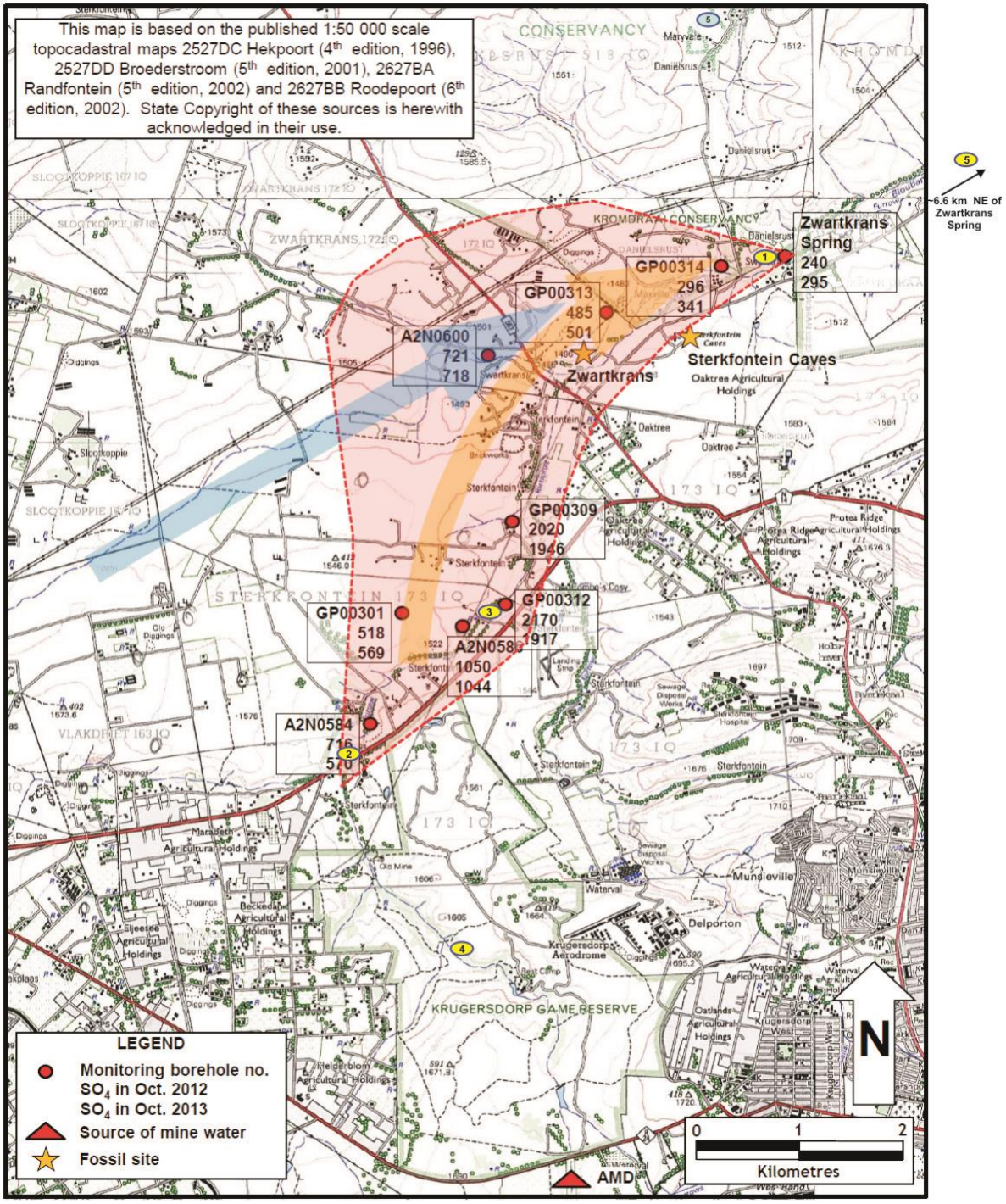

Figure 1: Locality map showing extent of study area and location of geophysical test sites (modified after Hobbs [2013])

The source of AMD occurs just south of the Krugersdorp Municipal Nature Reserve; the area of interest lies between the N14 and the Zwartkrans Spring – approximately 2 km north of the Sterkfontein Caves. The blue arrow indicates the principal direction of groundwater flow, while the orange arrow indicates the principal vector of allogenic recharge.

Table 2 is taken from the Year 1 year-end report and summarises the five test sites included in the study as well as the key groundwater quality information obtained/extracted from the ongoing borehole monitoring programme between 2013 and 2015.

Table 2: Salient descriptive information for each of the selected test sites

#	Test site	Proximity to existing borehole/spring	Other ground-truthing options	Water level (below ground level)	Known SO_4 levels of groundwater (mg/L)	Water conductivity (mS/m)
1	Boland Farm	~200 m from Zwartkrans Spring; ~300 m from GP00314	Smaller spring on ERT profile	~0–5 m?	**295** (Zwartkrans Spring – Oct 2013) **409** (Zwartkrans Spring – Dec 2015)	**124** (Zwartkrans Spring – Dec 2015) *103* (Local spring – March 2016)
2	Pinocchio's Farm	Private borehole 20 m from ERT profile	CSIR34/WBD2 ~80 m south of site	13 m (private borehole)	**661** (CSIR34/WBD2 – Sept 2013)	**137** (CSIR34/WBD2 – Sept 2013)
3	Crisuel Farm	GP00312 on ERT profile	–	6 m (GP00312, March 2016)	**1770** (GP00312, Dec 2015)	**300** (GP00312 – Dec 2015)
4	Krugersdorp Game Reserve (KGR)	GP00307 ~850 m from ERT profile	–	1.3 m (GP00307) ~10–15 m at ERT site	**1770** (GP00307, Dec 2015)	**253** (GP00307, Dec 2015)
5	Olwazini (Nedbank Training Centre)	Private borehole ~150 from ERT profile (just north of river)	–	Close to surface, 5–6 m?	No data yet	No data yet

The remainder of this report is divided into the following distinct sections or chapters:

- Chapter 2 provides an overview of the early project activities in Year 1; namely, a rock property study (Deliverable 1) and a model (simulation) study (Deliverable 2).
- Chapter 3 deals with an academic study conducted by S'bonelo Zulu, a student linked to the project. His MSc study focussed on the theoretical applicability of the time-lapse ERT survey approach to the stated hydro-geophysical problem and therefore provides an insightful introductory study to the subsequent sections.
- Chapter 4 details the repeat geophysical surveys (Deliverable 4), which were conducted in early 2017 and compares the results with the baseline surveys (Deliverable 3) that were conducted during Year 1.
- Chapter 5 includes some key concluding remarks as well as recommendations for the possible future application of geophysical monitoring involving the ERT method.

2 ROCK PROPERTY AND MODEL (SIMULATION) STUDIES

In Year 1, a rock property analysis of selected samples from the study area was conducted. A physical property analysis typically provides:

- A better understanding of the range of responses that may be observed during field surveys.
- An indication of whether a certain rock type has an exploitable anomalous physical property, compared to surrounding rocks.
- The basis for geophysical discrimination if the physical properties contrast.

Rock property information provides useful input to numerical model studies aimed at simulating realistic geoelectric scenarios. The property study conducted on the COH samples was based on a complex resistivity approach. In the complex resistivity approach, both the resistivity magnitude and the induced polarisation phase angle parameters are evaluated. This is done since most modern multi-channel resistivity meters are capable of measuring the resistivity and induced polarisation parameters simultaneously. The induced polarisation parameter is known to sometimes provide an added discrimination capability in geohydrological investigations.

The complex resistivity results for the COH samples are presented in Figure 2 and Figure 3.

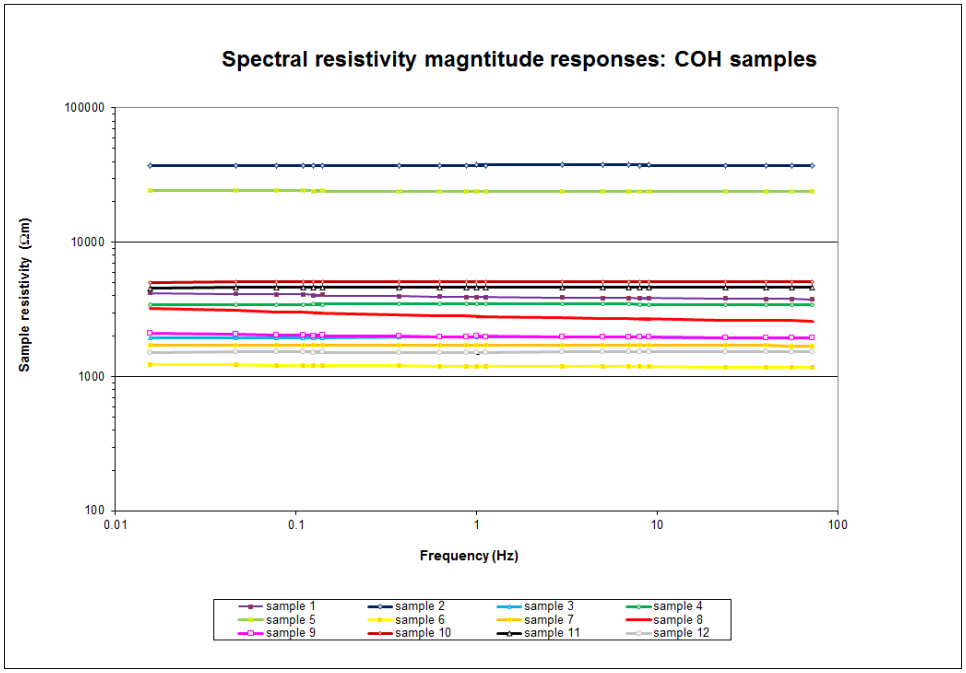

Figure 2: Resistivity magnitude vs. frequency plots for the COH samples

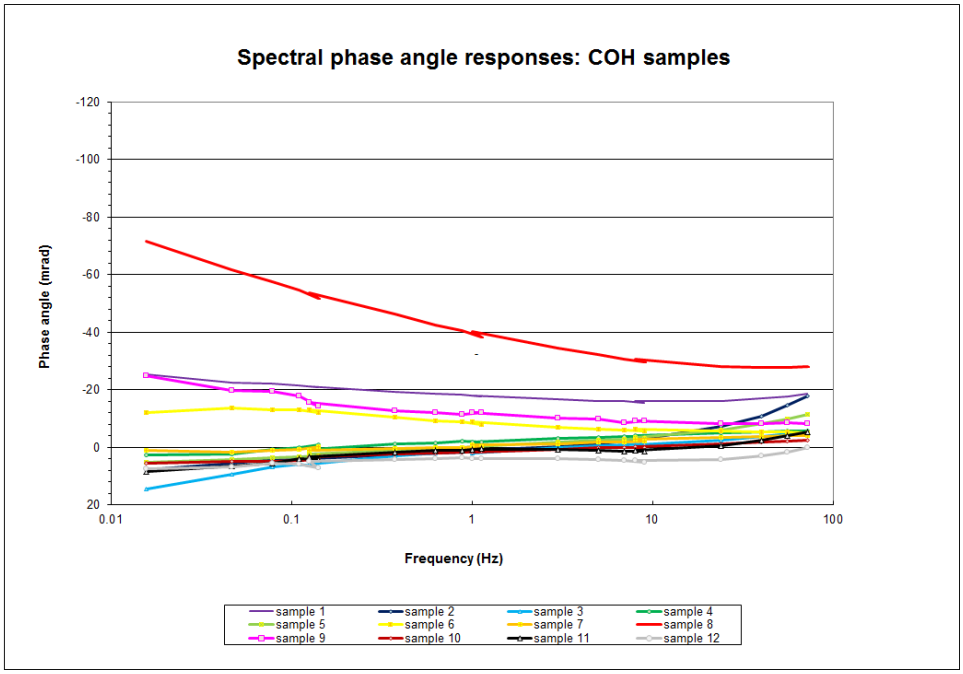

Figure 3: Phase angle vs. frequency plots for the COH samples

In summary, the sample resistivities were generally moderately high – within the range of 1200–5000 Ωm. Most samples showed little or no induced polarisation effect, with phase angle values typically ranging between 0 mrad and −8 mrad; these results provided useful background resistivity and phase angle model input parameter values for the subsequent model study.

The model study referred to above should not be confused with the model study conducted as part of the Year 2 activities, which is described in Chapter 3. The former was conducted in the early stages of the project and was aimed at determining appropriate survey and inversion parameters for the field surveys; the latter was part of a student project in Year 2 and was designed to assess the applicability of the time-lapse ERT approach.

The main objective of the Year 1 model study was to determine suitable field (acquisition) and inversion (imaging) parameters for the COH study. For example, the survey design was to be such that an effective depth of investigation of up to 30–40 m would be achieved easily. This target depth was based on the intention to focus on the upper portion of the shallow karst aquifer. As will be seen in Chapter 4, a deliberate attempt was made to select test sites where the top of the water table would be relatively close to surface (no more than approximately 20–25 m below surface). The motivation was simply to avoid the logistical burden of excessively long electrode spreads that would be required for deeper targets.

Another aim of this model study was to assess the suitability of the multi-gradient array measurement scheme that was selected. In the early stages of the project, it was still uncertain whether the acquisition of useful induced polarisation field data would be possible. The induced polarisation parameter is a very difficult parameter to record with a sufficiently high signal-to-noise ratio. This is because the magnitude of the induced polarisation related signal is extremely small compared to the resistivity magnitude, and it is also more subject to noise interference and unwanted coupling effects. The proposed multi-gradient array would in principle provide a better chance of obtaining useable induced polarisation data than the more commonly used dipole-dipole and Wenner arrays. Therefore, numerical modelling (computer simulations) was used to determine whether the multi-gradient array and associated measurement scheme would also provide adequate range and resolution capabilities.

The key findings of the simulations were that the multi-gradient array and associated measurement scheme involving a unit electrode spacing of 6–8 m would provide the required range and resolution and a better signal-to-noise ratio than more commonly used arrays.

3 TIME-LAPSE ERT MODEL STUDY

The model study described in this section was conducted later in the project, essentially between the baseline surveys of Year 1 and the repeat surveys of Year 2. As was mentioned earlier, this study focussed on the applicability of the time-lapse ERT survey approach.

In February 2017, S'bonelo Zulu submitted a research report at the University of the Witwatersrand for partial fulfilment of the Master of Science in Hydrogeology entitled *"The use of time-lapse electrical resistivity tomography to determine the footprint of acid mine drainage on groundwater"* (Zulu, 2017). The key aspects and findings of his study and the relevance to the Water Research Commission (WRC) K5/2440 project is summarised below. S'bonelo's research project was primarily a computer simulation study aimed at addressing a couple of pertinent questions around the application of the time-lapse ERT approach:

- Can time-lapse ERT identify the change in aquifer resistance as the pollution intensity changes over time?
- How sensitive is the time-lapse approach to subtle changes in pollution levels?

A brief summary of the research methodology and of key results are presented in the following sections. The approach followed by S'bonelo involved defining simple but realistic geoelectric models that might represent typical scenarios from the COH study area. Subtle perturbations to these models that represent changes in pollution levels over a given period were subsequently implemented and time-lapse ERT modelling applied. By comparing the before (perturbations) and after modelled ERT outputs as well as highlighting the differences between the respective outputs, it would then hopefully be possible to determine whether time-lapse ERT could detect the subtle model perturbations. By running a series of simulations for different scenarios, the sensitivity and applicability of the time-lapse approach could then be understood and quantified better. If the concept of time-lapse ERT proved to be applicable to the COH approach, it could ultimately be used to improve our understanding of the dynamic nature of the contamination footprint.

The geoelectric models used in the simulation study included the following basic scenarios:

- A thick layered aquifer (as part of a horizontally layered earth model).
- A more localised, wedge-shaped contamination zone.
- A vertical grike.
- A cavity.
- A thin lateral layer.
- A dipping grike.

For each model scenario, several perturbations involving changes to the aquifer properties were considered. For example, in the first perturbation, the resistivity ratio of the target layer was increased by a factor 5; in other words, the ratio of target resistivity to that of the same target in the baseline model was 1:5 (or 5 times more conductive). This would represent the most drastic (and probably easiest to detect) change in aquifer properties over time. Additional model perturbations for target resistivity ratios of 3:1, 2:1, 1.5:1, 1.2:1 and 1.1:1 were also considered. The last ratio of 1:1:1 represented the smallest (and most challenging) change to detect.

Example

To illustrate the above methodology using an example from the research project, consider the tomographic output image in Figure 4. This is the tomographic reconstruction of a layered earth model in which the middle conductive (blue) layer represents the aquifer layer with a resistivity of 50 Ωm. The two images in Figure 5 are the inversion outputs for the two extreme perturbations – for the largest (5:1) and smallest (1.1:1) contrast, respectively. Considering that the image scale values in ERT are not absolute, it is clear that it is virtually impossible to detect the simulated changes in aquifer properties by simply comparing either of the images in Figure 5 with the baseline equivalent in Figure 4 – even for a change ratio of 5:1.

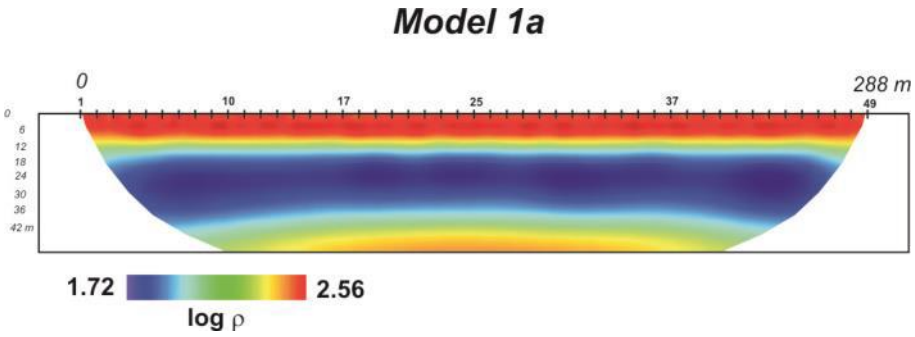

Figure 4: Example of a simulated baseline geoelectric model inversion result

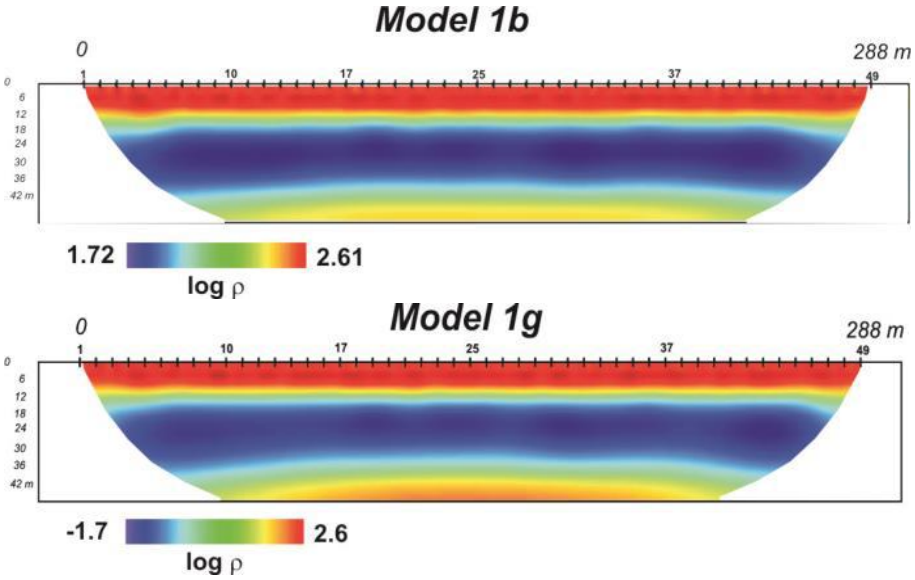

Figure 5: Selected inversion results for model perturbations

The time-lapse or difference imaging approach allows one to highlight the changes between the respective snapshot images, while suppressing those features in the image that do not change over time. The application of this approach is demonstrated in Figure 6 and the resulting outputs clearly only highlight the zones of interest (where transient change has occurred) in the model.

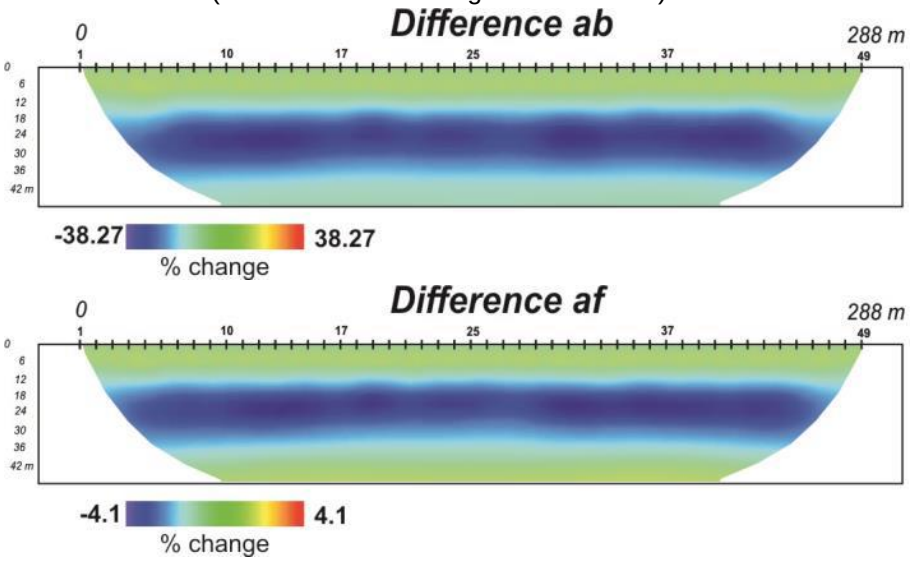

Figure 6: Difference imaging used to highlight the simulated transient changes between the baseline model (a) and Models b and f, respectively

The above example is proof that the time-lapse approach could work – even for very subtle target resistivity changes – in cases where the target comprises a significantly large volume of the sampled portion of the subsurface. However, to better assess the sensitivity of the approach, a number of smaller and more localised target scenarios were also considered in the model study. As an example, selected results for the thin vertical grike model are presented in Figure 7 and Figure 8. Here, three perturbations or target resistivity ratios of 5:1, 1.5:1 and 1.2:1 were considered.

In this example, the relative change from Model 3a to Model 3b, Model 3e and Model 3f is more evident, but it is difficult to visualise the exact nature of the change. However, the corresponding difference images (at least, Model 3ab and Model 3ae) reveal in a much clearer way the fact that the transient resistivity change is restricted to the vertical grike. The result for Model 3f is the first one in the sequence of model perturbations that is adversely affected by inversion artefacts; probably because the change in the target properties is of the same order as the random noise in the simulated data. This phenomenon was attributed to cases where the target (zone of change) becomes relatively small compared to the survey area.

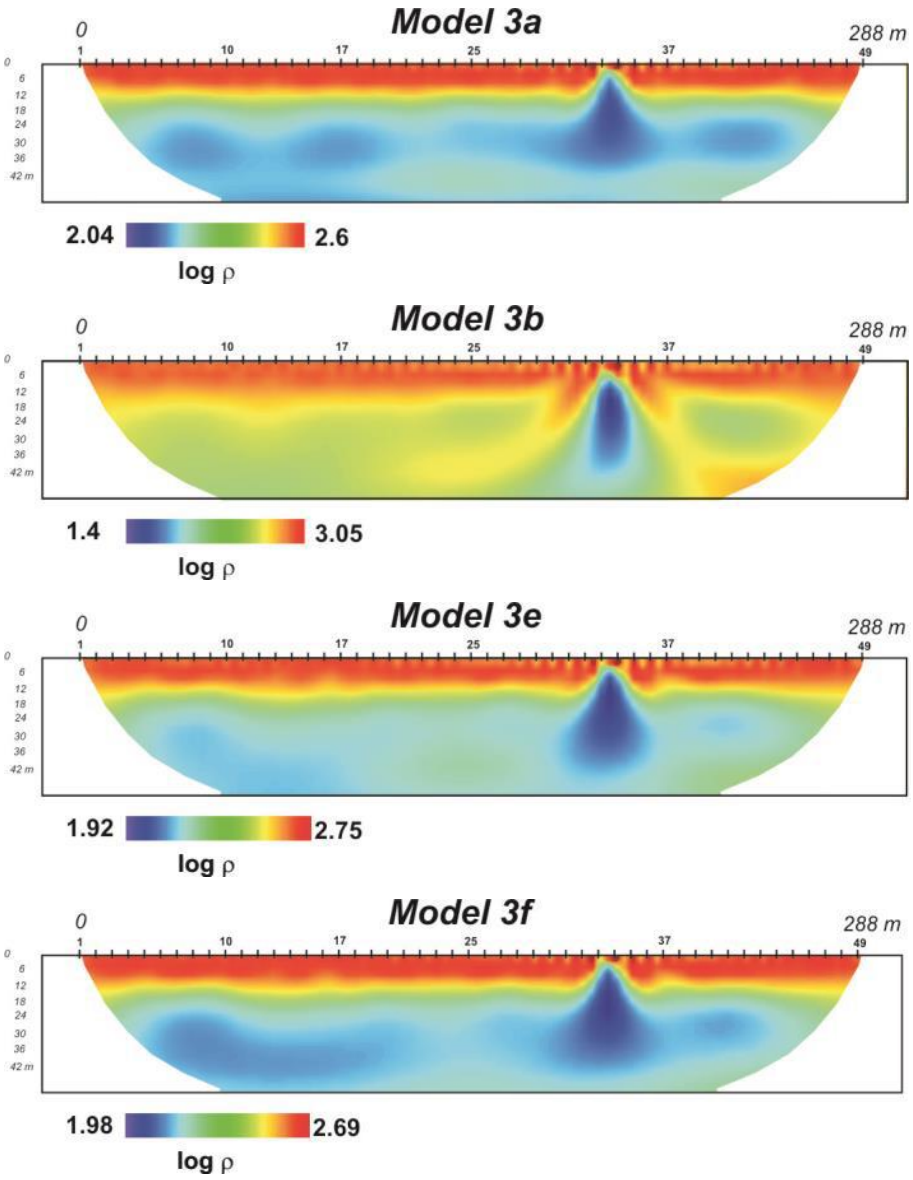

Figure 7: Inversion results for thin grike Model 3a and selected perturbations

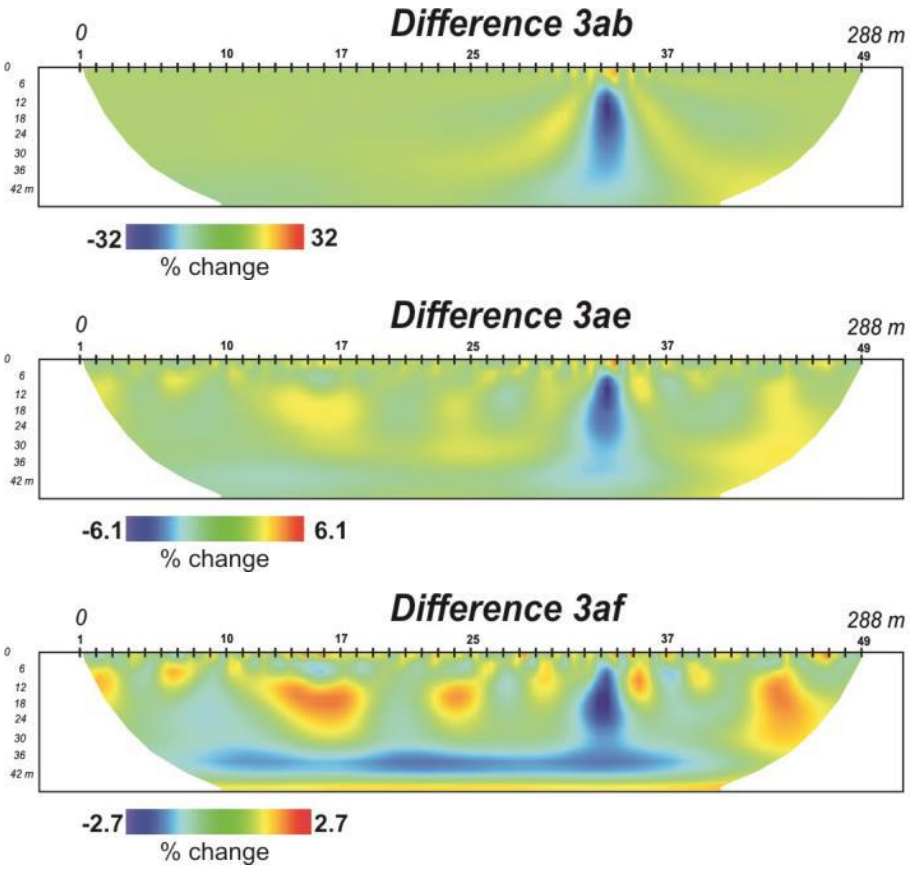

Figure 8: Selected difference imaging results for the thin grike model

The numerical model study concluded that the time-lapse ERT approach performed reasonably well in most cases; however, for more challenging scenarios it tended to fail. These failures were associated with cases where the changes in target resistivity were very small and/or where the target zones were located in low sensitivity parts of the survey area. The failure is characterised by distortions of the target area and the dominance of unwanted noise related artefacts. The best targets for the type of pollution monitoring attempted in the WRC project would be aquifers that could be associated with horizontal layers located relatively close to surface; that is, the top of the aquifer should not be so deep that it lies in a low sensitivity zone. The applicability of ERT to a specific problem scenario can be assessed using sensitivity maps (these can be calculated for the selected electrode configuration and measurement scheme). Numerical modelling can also be used to optimise ERT field parameters for a given scenario.

4 RECAP OF 2015/2016 ERT SURVEY RESULTS

A detailed discussion of the 2015/2016 ERT survey result appeared in the Year 1 final report. However, for the sake of context, the key results from that report is duplicated here to provide the foundation for any technical discussions that may flow out of the presentation of the repeat survey results in the subsequent chapter.

4.1 Site 1: Boland Farm

The Boland Farm site is located just north of the Sterkfontein Cave Road, close to the Zwartkrans Spring (Figure 9). A small local spring provides an excellent groundwater quality control option (in addition to the nearby Zwartkrans Spring), which also implies that the water table along the ERT profile is very close to the surface.

The ERT/induced polarisation data at Boland Farm was acquired on 9 and 10 December 2015. The inverted ERT resistivity magnitude image is shown in Figure 10. Figure 11 shows resistivity profiles

extracted from the ERT data for three different approximate depths. A total field magnetic profile measured along the same profile is also shown, for interest sake, in Figure 12.

Figure 9: Google Earth image of Site #1 – Van Rooy's Boland Farm (near Zwartkrans Spring and dyke)

The Sterkfontein Cave Road is seen in the lower right corner of the image with the Makiti Wedding Venue in the lower left corner; the ERT/induced polarisation profile is indicated by the yellow dotted line; the magenta dashed line indicate the anticipated strike of the Zwartkrans dyke; the light blue arrow shows the location of a local spring and the white arrow indicates the Zwartkrans Spring.

Discussion of results

The most prominent feature in the ERT image (Figure 10) is the highly resistive anomaly (red) near the centre of the spread (approximately between electrodes #22 and #27). This feature also appears to have high conductivity (low-resistivity) zones (blue) along its sides. These observations are consistent with the geophysical response of many intrusive dykes – the high resistivity corresponding to the actual dyke material and the high conductivities to the weathered sides of the dyke where it comes into contact with the host strata. A secondary prominent resistive anomaly is also observed between electrodes #11 and #15. It is not certain whether this anomaly is also associated with the dyke system. Unfortunately, no ground-truthing evidence, for example, outcrop or surface expression is available. Apart from these anomalies, the background resistivity appears to be fairly constant within the depth zone 8–20 m below surface, averaging approximately 70–90 Ωm.

The ERT image also reveals a high resistivity horizon at depths greater than approximately 25 m; these deeper structures are not actually relevant to the current study and will therefore not be analysed in any further detail. The surface layer in the ERT image appears to be relatively conductive, which can be attributed to the site being located on agricultural grazing land that would typically be associated with a loamier topsoil rather than an electrically resistive sandy overburden. Figure 12 also reveals evidence of the dyke in the form of a localised positive anomaly located between approximately $x \approx 120$ m and $x \approx 150$ m. However, the magnetic response along the ERT profile generally varies more than the resistivity-depth profiles. Also, some of the magnetic variations along this profile have higher relative amplitudes than the inferred dyke response.

Finally, an assessment of the in-field Boland Farm induced polarisation data quality (as well as that of subsequent surveys) showed that the signal-to-noise character of the phase angle response was not good enough to enable meaningful imaging. For this reason, only resistivity magnitude results are considered from this point onward.

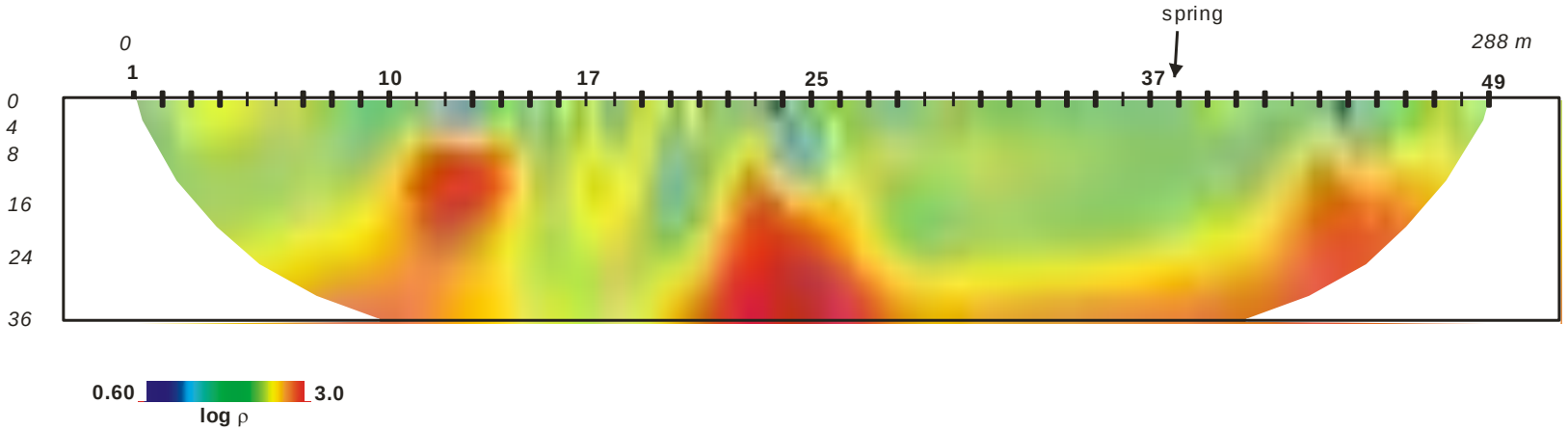

Figure 10: ERT output image for the Boland Farm site

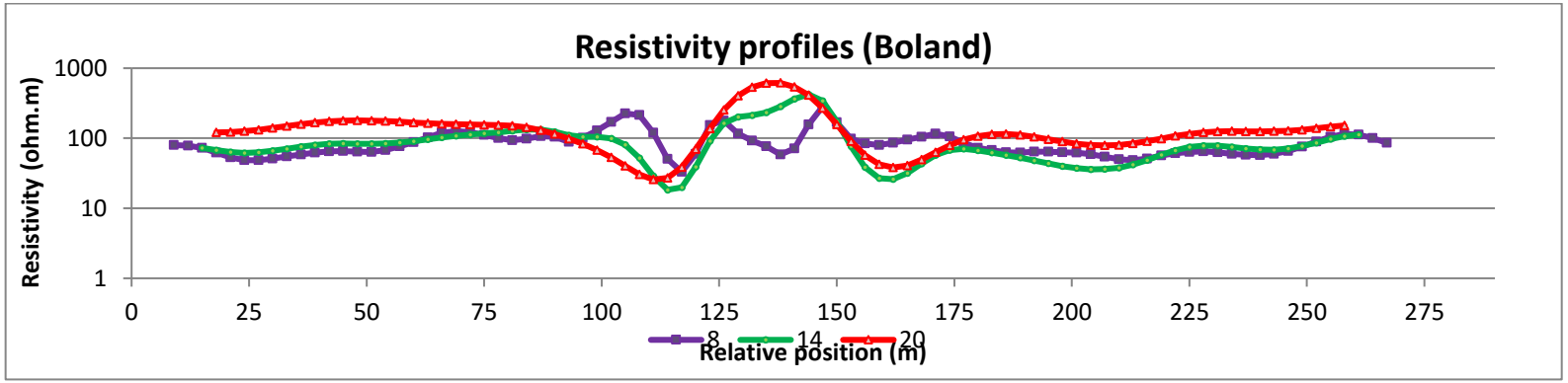

Figure 11: Resistivity-depth profiles for depths of 8 m, 14 m and 20 m below surface

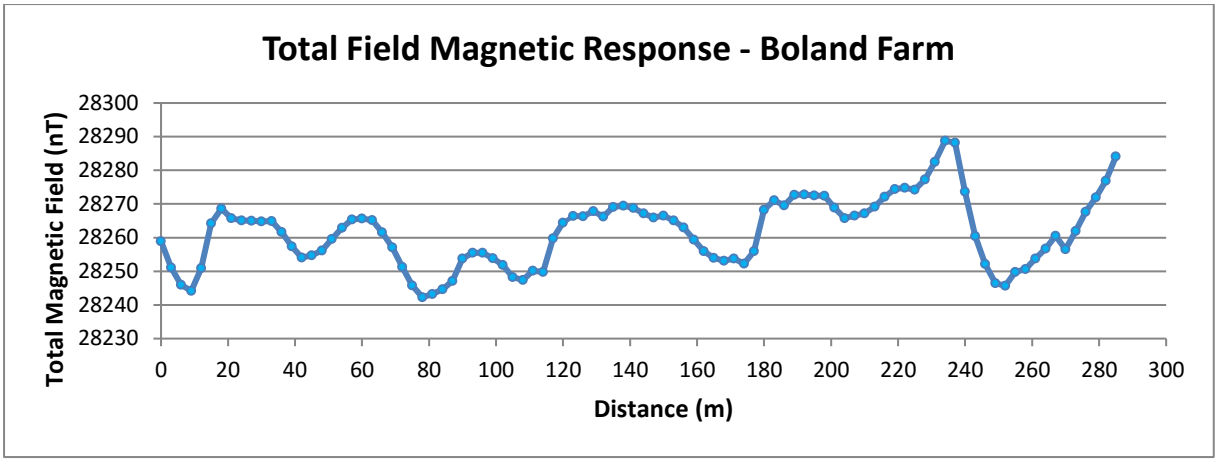

Figure 12: Total field magnetic response along the Boland ERT profile

4.2 Site 2: Pinocchio's Farm

Figure 13 shows the location of the ERT profile at Pinocchio's Farm, which is close to a private borehole that could be used as a water quality control point. Another borehole (CSIR34/WBD2) is also located less than 100 m away on the southern side of the N14. This borehole was last sampled in October 2013 when the borehole water conductivity was recorded at 137 mS/m. Unfortunately, it was not possible to sample the private borehole during this study.

Figure 13: Google Earth image of the Pinocchio's Farm site next to the N14

The N14 is seen extending in a SW–NE direction across the image; the ERT profile is indicated by the yellow line; the blue arrow indicates a known private borehole that is available for monitoring purposes; the red marker shows the location of the nearest alternative monitoring borehole CSIR34/WBD2.

The data acquisition was conducted on 27 January 2016 and the ERT inversion result is presented in Figure 14. Figure 15 shows the resistivity profiles extracted from the ERT data for three different depths. A total field magnetic profile measured along the ERT profile is shown in Figure 16.

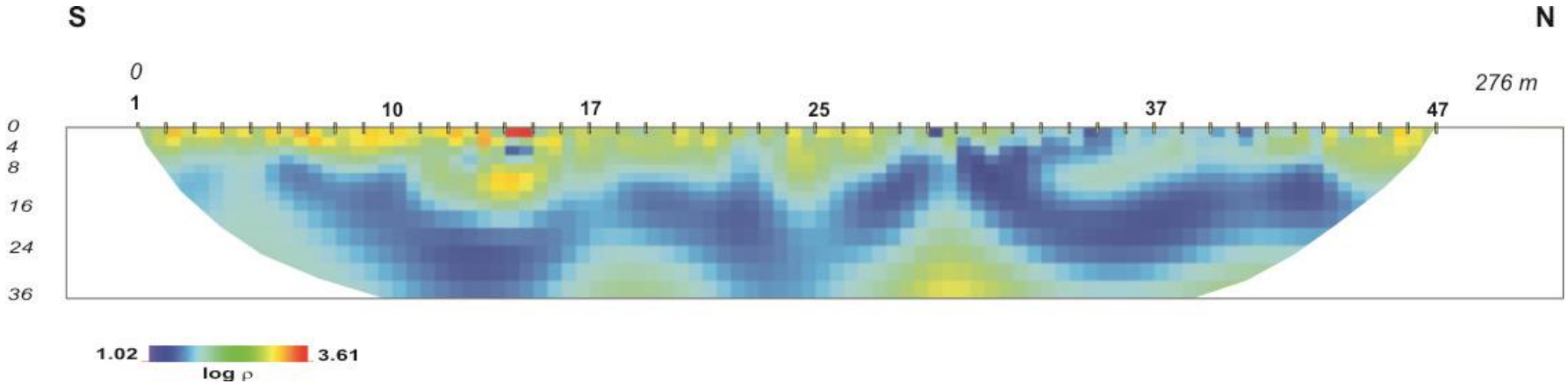

Figure 14: ERT output image for the Pinocchio's Farm site

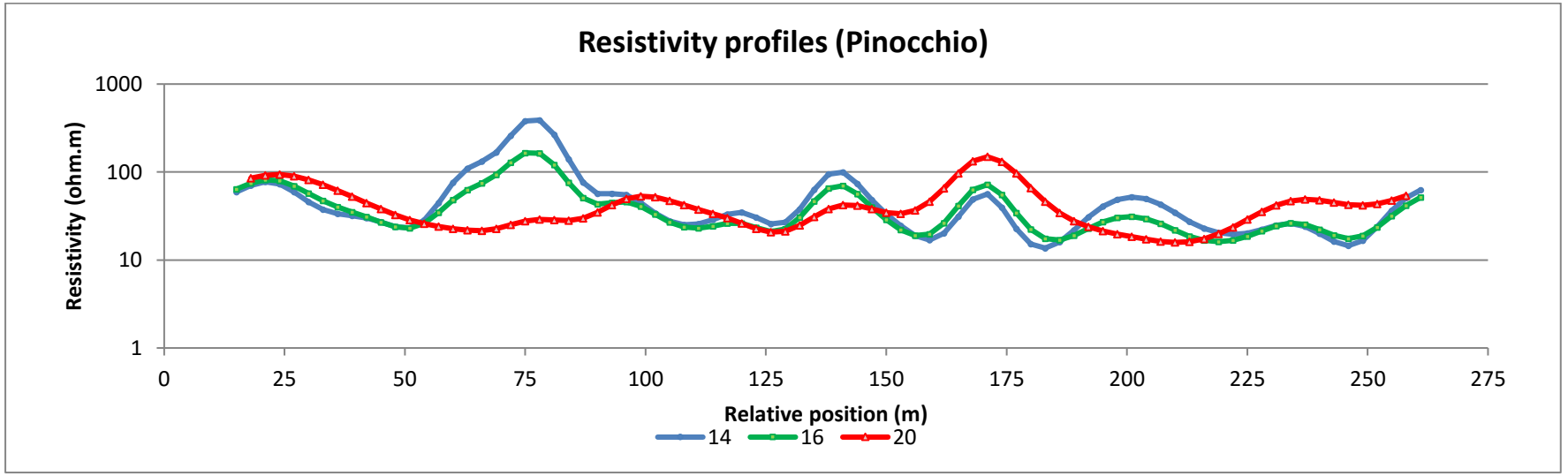

Figure 15: Resistivity-depth profiles for depths of 14 m, 16 m and 20 m below surface (Pinocchio)

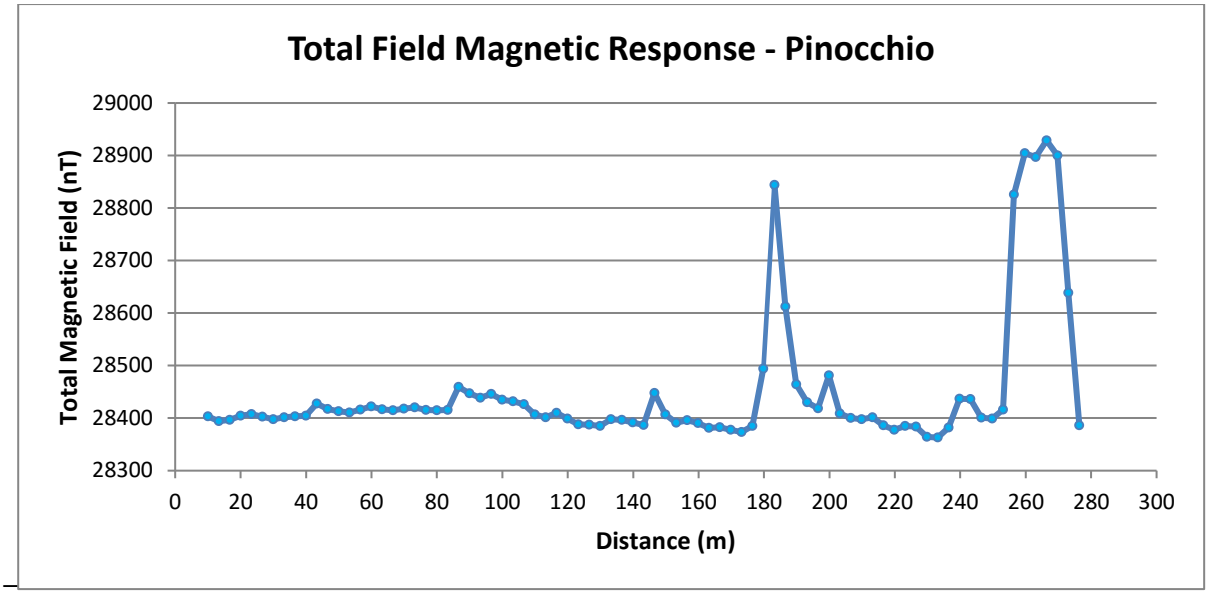

Figure 16: Total field magnetic response along the Pinocchio's Farm ERT profile

Discussion of results

The ERT output image reveals a highly conductive (dark blue) layer that extends from the very near surface down to depths of more than 30 m. This conductive zone is inferred to represent the local karst aquifer, which is expected to contain fairly contaminated groundwater. The depth to the top of this layer appears to vary between about 8 m and 16 m; this correlates well with the known water table depth at the previously mentioned private borehole, which was measured as 13.3 m in March 2016. This borehole is located within approximately 5 m of the ERT line and between electrodes #39 and #40.

The resistivity-depth profiles in Figure 15 indicate that the average background resistivity at depths of a few metres below the water table is of the order of 20-40 Ωm and shows some lateral variations within this range. It is uncertain whether the apparent local high resistivity anomaly located at approximately x = 80 m is associated with a geological structure of some sort, but there is no evidence of this in the magnetic profile (Figure 16).

The magnetic profile shows two significant anomalies at x = 180–190 m and x = 260–270 m. The former could be correlated with the minor resistivity high seen in the resistivity-depth profiles at approximately x = 180 m. Like the magnetic data, the ERT image suggests that this structure is possibly very thin and flanked by high-contrast low-resistivity material. The cause of the second magnetic anomaly that occurs towards the end of the profile cannot be positively correlated with any feature in the ERT data as the last ERT electrode more or less coincided with the peak of this anomaly.

4.3 Site 3: Crisuel Farm

The site on Crisuel Farm was located right next to Department of Water and Sanitation (DWS) monitoring borehole GP00312 (Figures 17). The ERT survey was conducted on 11 February 2016. The two-dimensional profile extends more or less from this borehole in a south-westerly direction towards the farmhouse. The #1 electrode is located right on the edge of the stream in the south-west, with the last electrode, in this case #47, located approximately 10 m to the north of borehole GP00312. A unit electrode spacing of 6 m was used, resulting in a total spread length of 276 m. Figure 18 shows the inverted ERT output image, while Figure 19 shows the resistivity profiles extracted from the ERT data for three different depths. A total field magnetic profile measured along the ERT profile is shown in Figure 20.

Figure 17: Google Earth image of the Crisuel Farm site next to the N14

The N14 is seen extending in a SW–NE direction across the right of the image; the ERT profile is indicated by the yellow dotted line; the blue arrow indicates the location of borehole GP00312.

Discussion of results

The ERT output image indicates two distinct near-surface zones along the profile. From electrode #1 (beside the stream) up to approximately electrode #19, the near-surface resistivity proved to be relatively low. It was also evident from the field observations that the average resistivity decreased rapidly as one approached the stream and electrode #1. From approximately electrode #20 to the north-eastern end of the profile, the near surface was very resistive and injecting current into the subsurface proved to be challenging. These trends in subsurface resistivity are also evident in the individual resistivity-depth plots presented in Figure 19. The rapid change in bulk resistivity – especially to the west of electrode #19 – is possibly related to a paleo sinkhole structure as evidence of this (for example previous subsidence) can be seen on surface. The sudden change reflected in the resistivity data can also be seen in the corresponding magnetic data (Figure 20), with a sudden decrease in magnetic values occurring at approximately x = 90–110 m as one moves north-east along the profile.

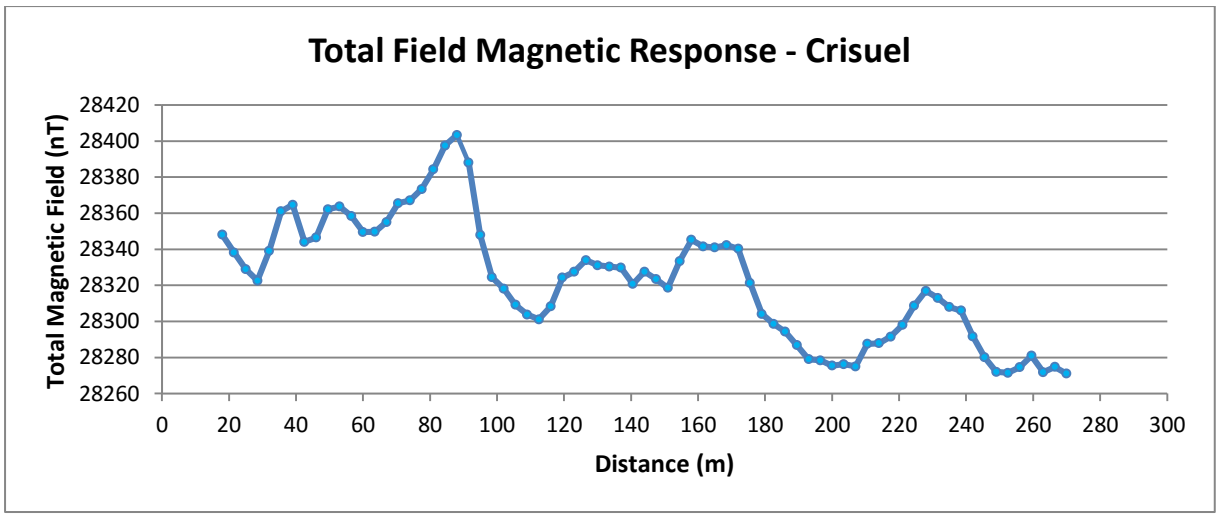

Figure 18: Total field magnetic response along the Crisuel ERT profile

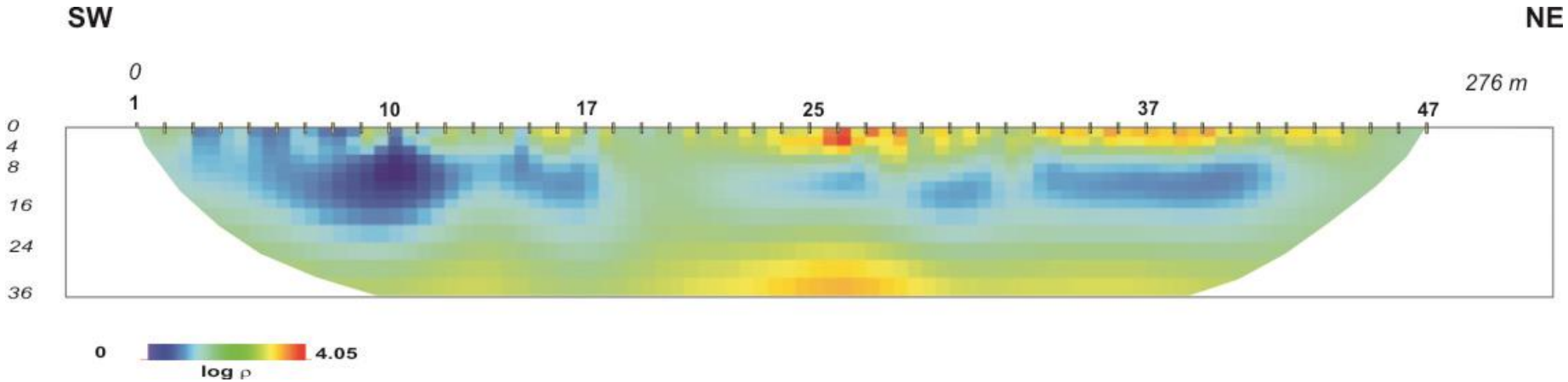

Figure 19: ERT output image for the Crisuel Farm site

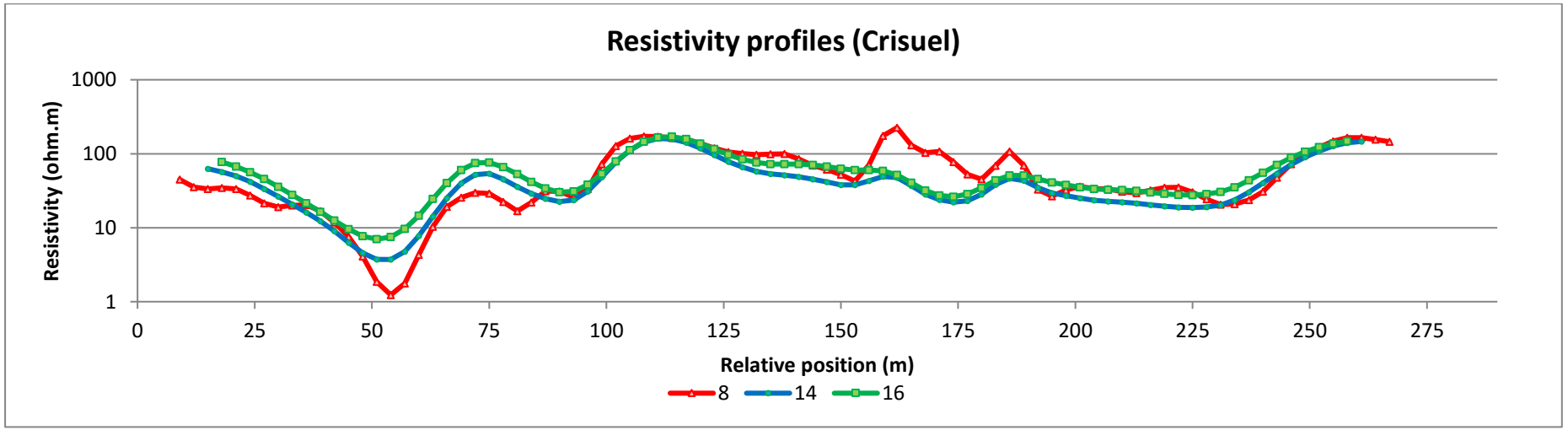

Figure 20: Resistivity profiles for depths of 8 m, 14 m and 16 m below surface (Crisuel)

4.4 Site 4: Krugersdorp Game Reserve

The KGR site is located just east of the south-eastern corner of the reserve's Lion Camp (Figure 21). The ERT profile was located with electrode #49 approximately 64 m from the corner of the Lion Camp; electrode #1 was located at the eastern extreme of the profile. A unit electrode spacing of 7 m was used, resulting in a total spread length of 336 m. The survey was conducted on 02 March 2016.

Figure 22 shows the inverted ERT output image and Figure 23 shows the resistivity profiles extracted from the ERT data for three different depths. A total field magnetic profile measured along the ERT profile is shown in Figure 24.

Figure 21: Google Earth image of the KGR ERT site

The Lion Camp of the KGR is seen at the top left of the image; the ERT profile is indicated by the yellow dotted line; the electrode defined as #1 during the survey is located at the eastern end of the profile and electrode #49 is located approximately 64 m from the corner of the Lion Camp.

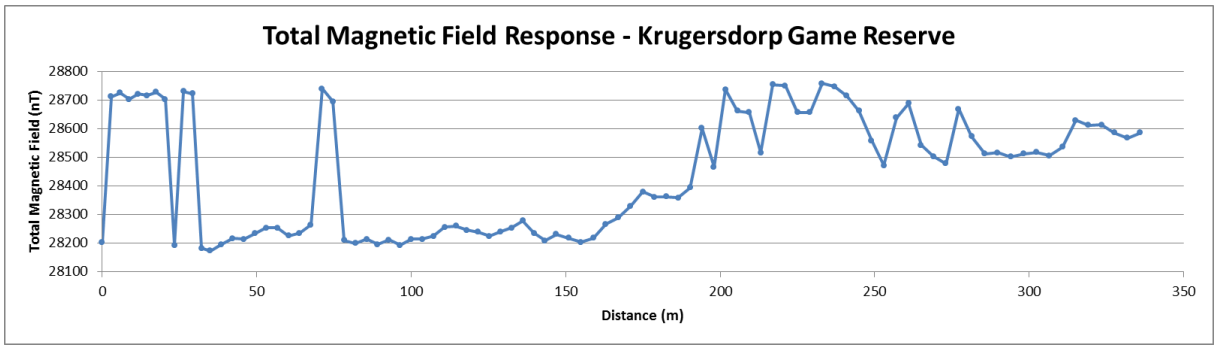

Figure 22: Total field magnetic response along the KGR ERT profile

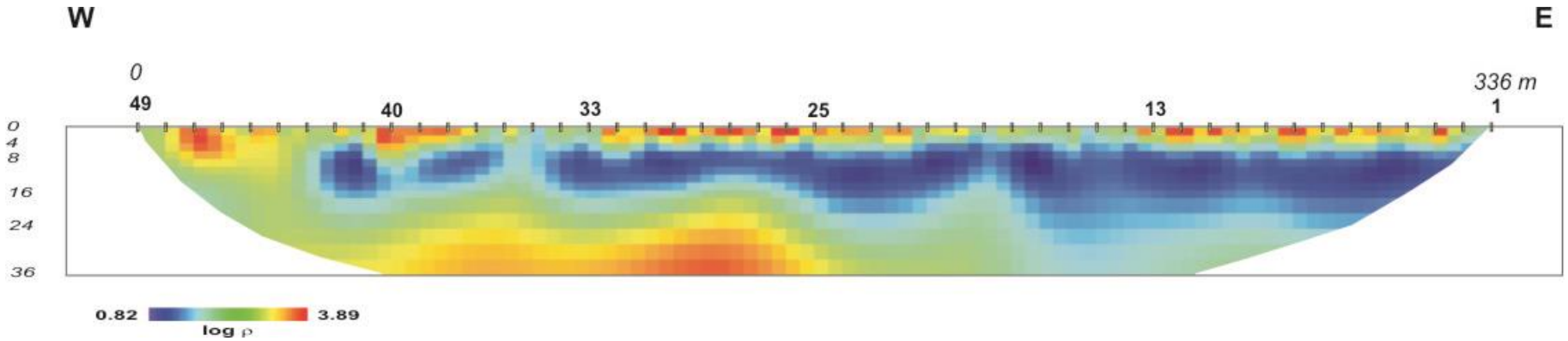

Figure 23: ERT output image for the KGR site

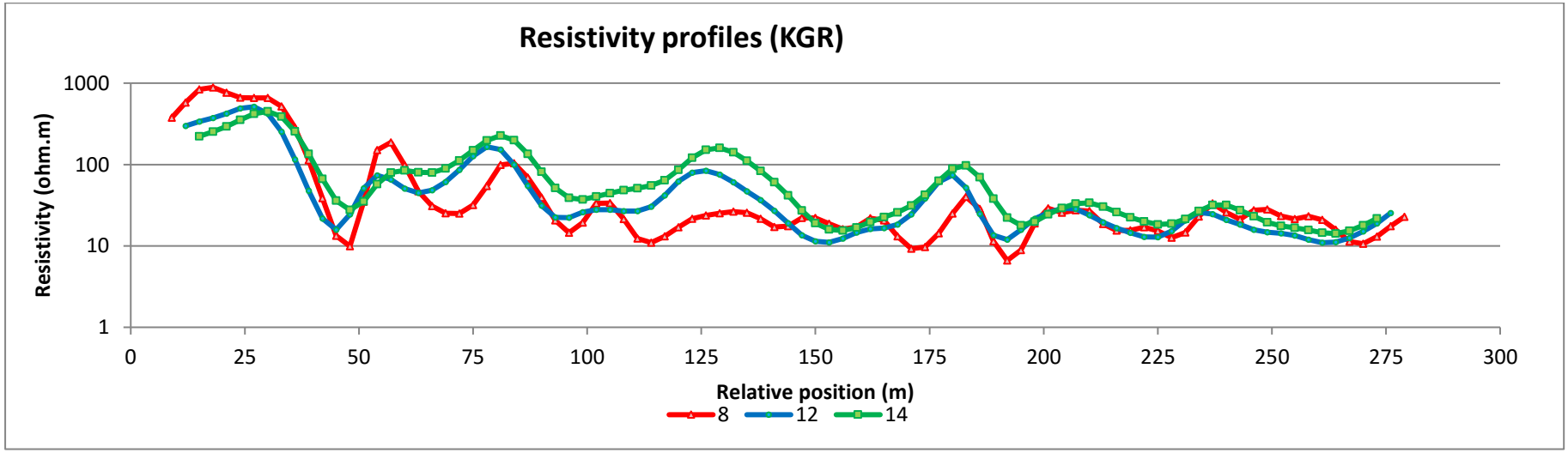

Figure 24: Resistivity profiles for depths of 8 m, 12 m and 14 m below surface (KGR)

Discussion of results

The ERT output image shows a fairly resistive surface layer, which was also reflected by in-field difficulties in injecting current into the ground. In some places, especially towards the eastern side of the spread, there was evidence of very shallow hard rock (almost outcropping), which would possibly further contribute to the high near-surface resistivity. Immediately below the high resistivity surface layer is a band of very low resistivity that extends virtually across the whole extent of the ERT spread. From west to east, the survey is inferred to proceed from the Oaktree Formation of the Malmani Subgroup dolomite onto the older Black Reef Formation (mainly quartzites). This circumstance might explain the 'step' in the total field magnetic response located between ~150 m and ~200 m (Figure 24) along the traverse.

It is postulated that the increase in the thickness of the conductive zone at the eastern end of the traverse might reflect water ingress from the proximal Tweelopie Spruit into the Black Reef Formation quartzites. This location is located relatively close (< 2–3 km) to the AMD source. The gradually decreasing trend in the resistivity from west to east can also be seen in the individual resistivity profiles (Figure 23).

4.5 Site 5: Olwazini (Nedbank) Property

The ERT site at Olwazini is shown in the Google Earth image in Figure 25. This site was chosen as a control site; in other words, a site where the impact of the AMD contamination is not expected to manifest and for which the groundwater quality is expected to remain relatively unchanged over time, compared to those sites that is affected by AMD. Olwazini is located approximately 6.6 km north-east of the Zwartkrans Spring area and is therefore far enough away from the inferred AMD footprint (refer to Figure 1) to not be contaminated with AMD sulphates.

ERT data acquisition was conducted on 31 March 2016. A 6 m unit electrode spacing was employed, using a total of 49 electrodes. The total length of the electrode spread was 276 m. Figure 26 shows the inverted ERT output image and Figure 27 shows the resistivity profiles extracted from the ERT data for three different depths. A total field magnetic profile measured along the ERT profile is shown in Figure 28.

Figure 25: Google Earth image of the Olwazini site

Nedbank's Olwazini complex located alongside the R374 is seen at the bottom left of the image; the ERT profile is indicated by the green line just south of the river

Discussion of results

The ERT output image (Figure 26) reveals a highly conductive surface layer (blue) that generally extends down to a depth of no more than about 6 m; in some locations – close to the western and eastern ends of the profile and also near electrode #35–36 – this geoelectric layer appears to extend a few metres deeper. This conductive layer would be consistent with agricultural soil that is regularly irrigated and cultivated. The layer of intermediate resistivity (green-yellow) is inferred to be associated with the karst aquifer. The highly resistive (red) basal layer is thought to be associated with either underlying older Witwatersrand sediments or a less weathered and more resistive dolomitic unit such as the basal Oaktree Formation.

The only anomalous structure that is evident in the ERT and also in the magnetic data is located beneath electrodes #3 and #4; this relatively conductive feature is also associated with a significant (> 300 nT) low magnetic anomaly (Figure 28). It is not certain whether this feature is associated with a geological structure but it could also be the response of a man-made structure or utility such as a drain pipe. The quality of the ambient groundwater still needs to be established.

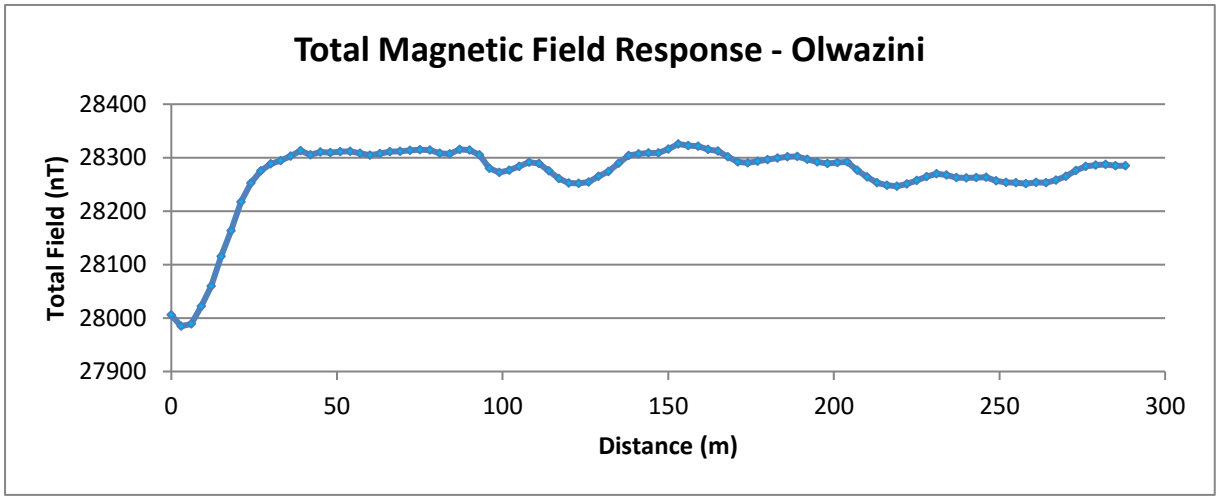

Figure 26: Total field magnetic response along the Olwazini ERT profile

4.6 Summary

The ERT surveys of Year 1 targeted a variety of sites representing a spectrum of pollution scenarios in the COH study area. At the one extreme was highly contaminated aquifer sites (e.g. Pinocchio and Crisuel) with sulphate levels exceeding 1500 mg/L; at the other extreme, a control site at Olwazini is characterised by groundwater that is not expected to be significantly affected by AMD. The primary aim of the geophysical surveys was to characterise and quantify the electrical resistivity of the dolomitic aquifer and to establish baseline geophysical 'snap shots' for these test sites. Table 3 summarises the key groundwater quality information obtained/extracted from the ongoing borehole monitoring programme and the geophysical surveys conducted in Year 1.

The ultimate objective of the project was to revisit these sites after approximately 12 months and repeat the resistivity surveys. Transient changes in the groundwater quality – in particular the sulphate concentration – are expected to possibly manifest as corresponding changes in the baseline resistivity responses. These repeat surveys were done between March 2017 and June 2017 and are described in the section that follows.

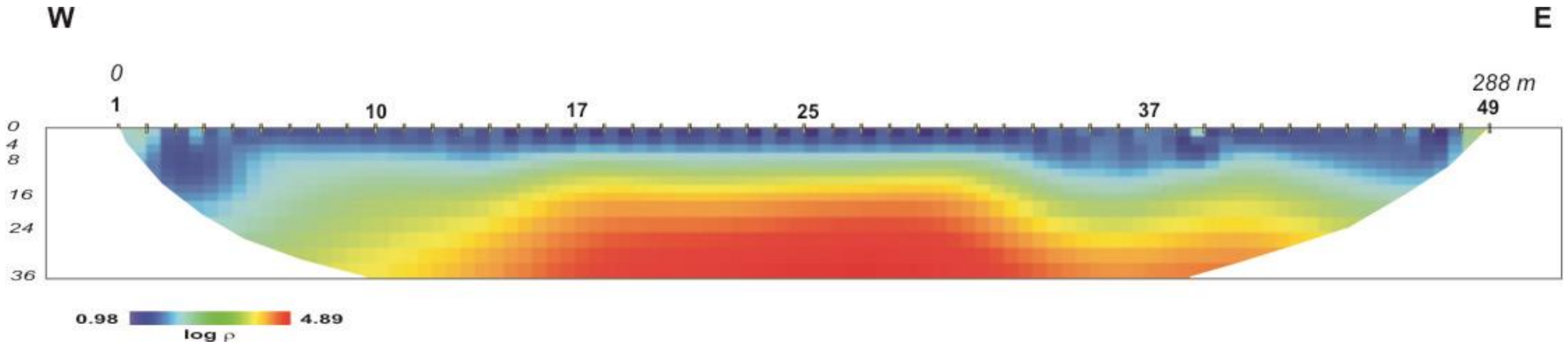

Figure 27: ERT output image for the Olwazini site

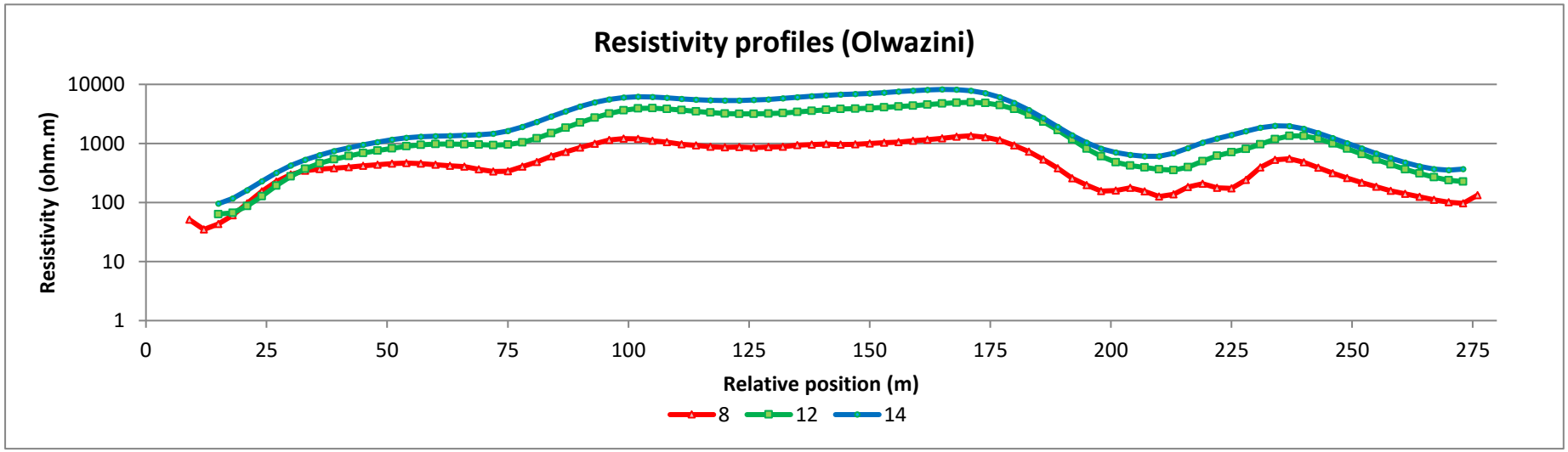

Figure 28: Resistivity profiles for depths of 8 m, 12 m and 14 m below surface (Olwazini)

Table 3: Test sites and summary of relevant chemical hydrogeology and geophysical results

#	Test site	Water level (below ground level)	Known SO_4 levels of groundwater (mg/L)	Water conductivity (mS/m)	Estimated resistivity range of aquifer inferred from ERT data (Ωm)
1	Boland Farm	~0–5 m?	**295** Zwartkrans Spring – Oct 2013) **409** (Zwartkrans Spring – Dec 2015)	**124** (Zwartkrans Spring – Dec 2015) *103* (Local spring – March 2016)	40–90
2	Pinocchio's Farm	13 m (private borehole)	**661** (CSIR34/WBD2 – Sept 2013)	**137** (CSIR34/WBD2 – Sept 2013)	20–50
3	Crisuel Farm	6 m (GP00312, March 2016)	**1770** (GP00312 – Dec 2015)	**300** (GP00312 – Dec 2015)	20–90
4	KGR	~5–10 m	**1770** (GP00307)	**253** (GP00307)	10–50
5	Olwazini (Nedbank Training Centre)	Close to surface, 5–6 m?	No data yet	No data yet	100–1000

5 REPEAT ERT SURVEYS – YEAR 2

The repeat ERT surveys were originally planned for around March 2017 to ensure that the elapsed time between the Year 1 and Year 2 surveys would be maximised (at least 12 months). However, during survey attempts in March 2017 at Boland Farm, equipment problems were experienced, which resulted in the start of the repeat survey campaign being delayed by approximately two months. Ultimately, all five repeat surveys were conducted during June 2017. Results for these five surveys are described and discussed below.

5.1 Boland Farm Repeat Survey

The Year 2 Boland Farm ERT survey was conducted on 2 June 2017, which was 541 days or approximately 18 months after the original baseline survey in December 2015. Exactly the same field configuration was used as in the Year 1 survey and special care was taken to relocate the electrode positions with as much accuracy as possible. To achieve this, field notes and photographs of the 2016 field set-up were consulted. The same measurement scheme used in 2016 was also applied. These steps aimed at conducting the survey under the same conditions as 2016 and the same field parameters as in Year 1 were subsequently also applied at all other test sites. The results are shown in Figure 29.

Unfortunately, the Boland repeat survey produced results for which a thorough reprocessing of Year 1 and Year 2 results was strongly advised after the initial evaluation of the results and before any further inferences relating to these images could be made with a fair degree of confidence. The uncertainty related to the fact that, despite some gross similarities, the differences between the Year 1 and Year 2 results were more extreme than expected. These discrepancies were reported and discussed at the September 2017 Reference Group meeting. Subsequent to the Reference Group meeting, the data quality control, data processing and tomographic reconstruction processes for both Boland Farm data sets were revisited. However, even though more stringent data quality control measures were applied, the similarity between the Year 1 and Year 2 results was still not as evident as it proved to be in some of the results from other test sites. The updated results are compared in Figure 29. The prominent resistive anomaly in the central part of the Year 1 image, which was attributed to the inferred presence of the Zwartkrans dyke, does not appear to manifest clearly in the Year 2 image. Additionally, the secondary prominent resistive feature (around electrodes #11–15 in the Year 1 image) appears to be somewhat distorted and even shifted towards electrode #17 in the Year 2 image.

The likelihood of electrode relocation errors in Year 2 playing a role in the above discrepancies was considered as a possible cause; however, the impact of such errors at Boland Farm was expected to be low, unless the subsurface geological structures (for example, associated with the inferred dyke), changed very rapidly over short distances. Significant transient changes in the near-surface geoelectric structure; for example, as a result of seasonal effects, could also have contributed to the apparent discrepancies between Year 1 and Year 2 results.

A final possibility was considered, namely, that of compromised cables, particularly during the Year 1 survey. Damaged cables were discovered shortly after the initial Boland Farm survey and were repaired/replaced at the time. If some take-out combinations were not functioning as expected during the Boland Farm baseline survey, undetected systematic errors may have been introduced into the data, which could easily manifest as artefacts and/or distorted resistivity anomalies in the output images. Unfortunately, such systematic errors are difficult to detect during surveys and therefore difficult to correct for after the fact.

Lessons learnt from the above experience include the consideration of survey strategies aimed at minimising/eliminating electrode relocation errors as well as systematic errors caused by, for example, equipment-related malfunction. Ideally, one should employ permanent electrodes in time-lapse studies so as to eliminate electrode location errors completely, but this was not possible within the scope of these experimental surveys. To address the issue of systematic errors, it is advised to implement survey strategies aimed at identifying possible systematic errors and better quantifying the noise in the data. This can be done using reciprocal measurements; however, this approach is typically time-consuming

as it effectively means an approximate doubling in survey time. It is therefore recommended that any future similar survey efforts involve using fast-sampling automated resistivity systems to overcome this constraint.

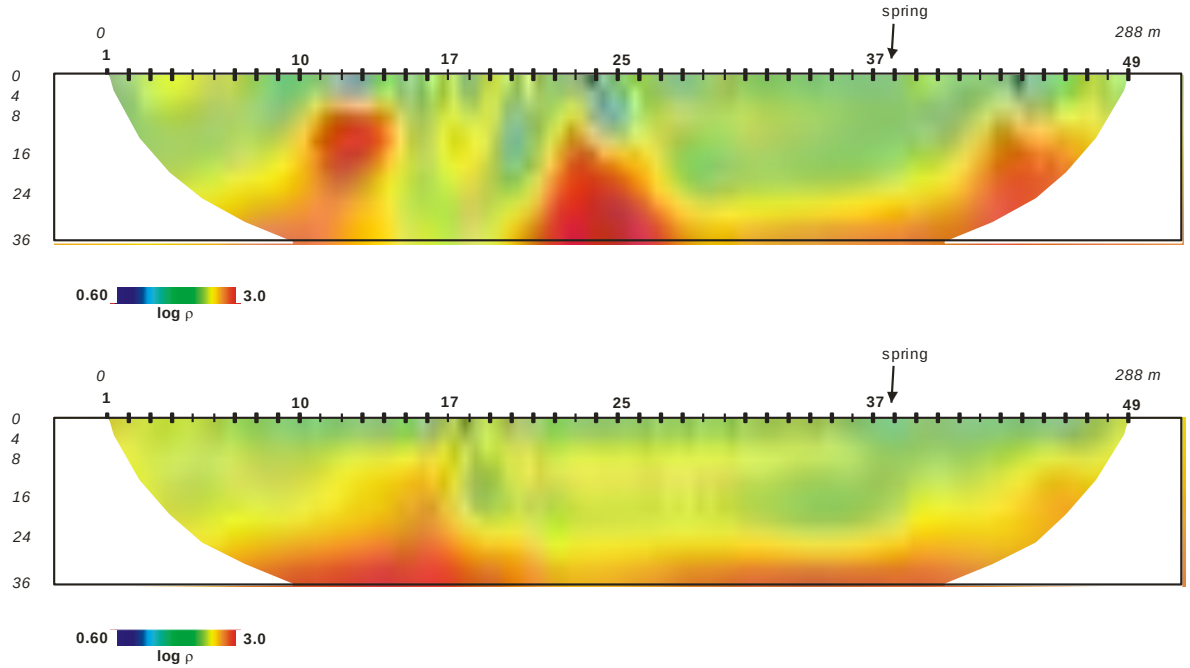

Figure 29: Results of the 2017 Boland Farm repeat survey and comparison with Year 1 result

5.2 Pinocchio's Farm Repeat Survey

The Pinocchio's Farm repeat survey was conducted on 8 June 2017, 498 days or just more than 16 months after the original survey. As before, care was taken to relocate the electrode positions with as much accuracy as possible and to use the same measurement scheme as Year 1. The tomographic inversion results are shown in Figure 30. The top image is the Year 1 result, the middle image the Year 2 result, while the bottom image depicts the relative change, which is presented as a percentage change in the estimated pixel resistivity log values. Selected resistivity-depth profiles are shown in Figure 31 and are compared to the equivalent Year 1 profiles.

The Year 2 ERT image (Figure 30) reveals the same highly conductive (dark blue) zone that extends virtually across the entire image, ranging from depths close to surface to more than 30 m below surface in places. This conductive band was previously attributed to the contaminated local karst aquifer.

The resistivity-depth profiles in Figure 31 suggest relatively little change at the selected depths across most of the electrode spread, except for two distinct exceptions (at around 75 m and again at around 210 m). At these locations, fairly significant changes in resistivity (nevertheless, relatively shallow and localised) appear to have occurred over time.

An attempt to compare the ERT results to borehole information was limited to available data from a borehole (GP00302) located a few hundred metres downstream. Even though this borehole was not the first choice or closest option for this comparison, it would nevertheless provide a useful indication of how the local groundwater quality changed over the study period. In December 2015, GP00302 had a sulphate level of ~1400 mg/L and an electrical conductivity level of ~220 mS/m). By July 2016, these values had changed to 1520 mg/L and 250 mS/m, respectively. Shortly before the repeat survey in February 2017, the sulphate level had increased further to 1640 mg/L, with an electrical conductivity of 255 mS/m.

If one ignored the two localised anomalies mentioned above, and only focussed on the background resistivity profiles in Figure 31, it is not possible to unequivocally correlate the gradual increase in sulphate level between late-2015 and mid-2017 with an anticipated negative background resistivity

difference for the aquifer; an increase in sulphate content is expected to be associated with an increase in conductivity (as is also reflected in the borehole electrical conductivity values); that is, a decrease in resistivity. For example, the average background level for the Y2–Y1 curves in Figure 31 seems to be near-zero but is also characterised by minor oscillations around the zero level. These oscillations can be attributed to resistivity variations within the associated portion of the aquifer. It can be inferred that the gradual increase in local aquifer sulphate level over the study period (equating to ~7%) does not translate to a large enough change in the bulk aquifer resistivity response to be detectable in practice.

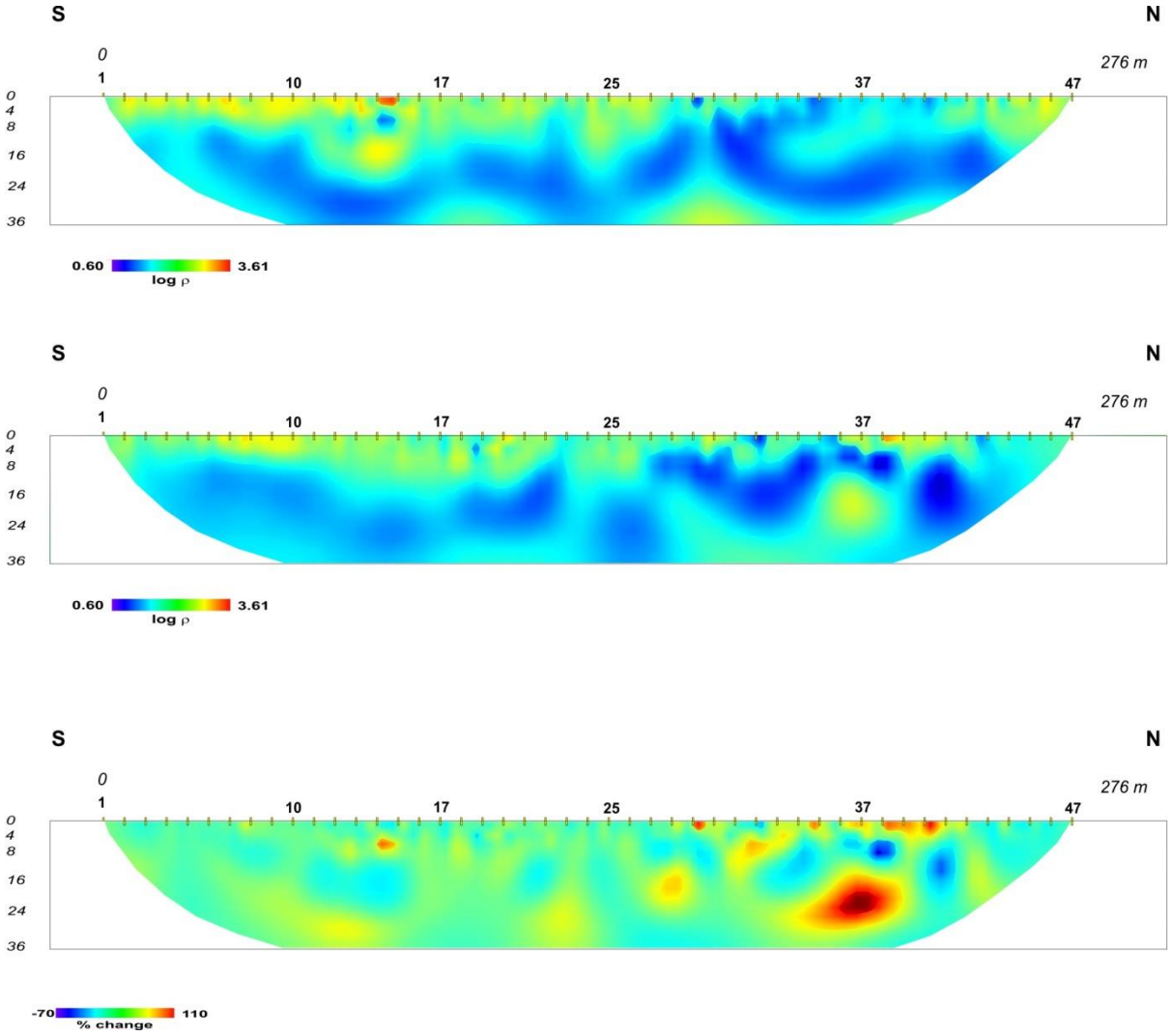

Figure 30: Results of 2017 repeat survey at Pinocchio's Farm and comparison with Year 1 result

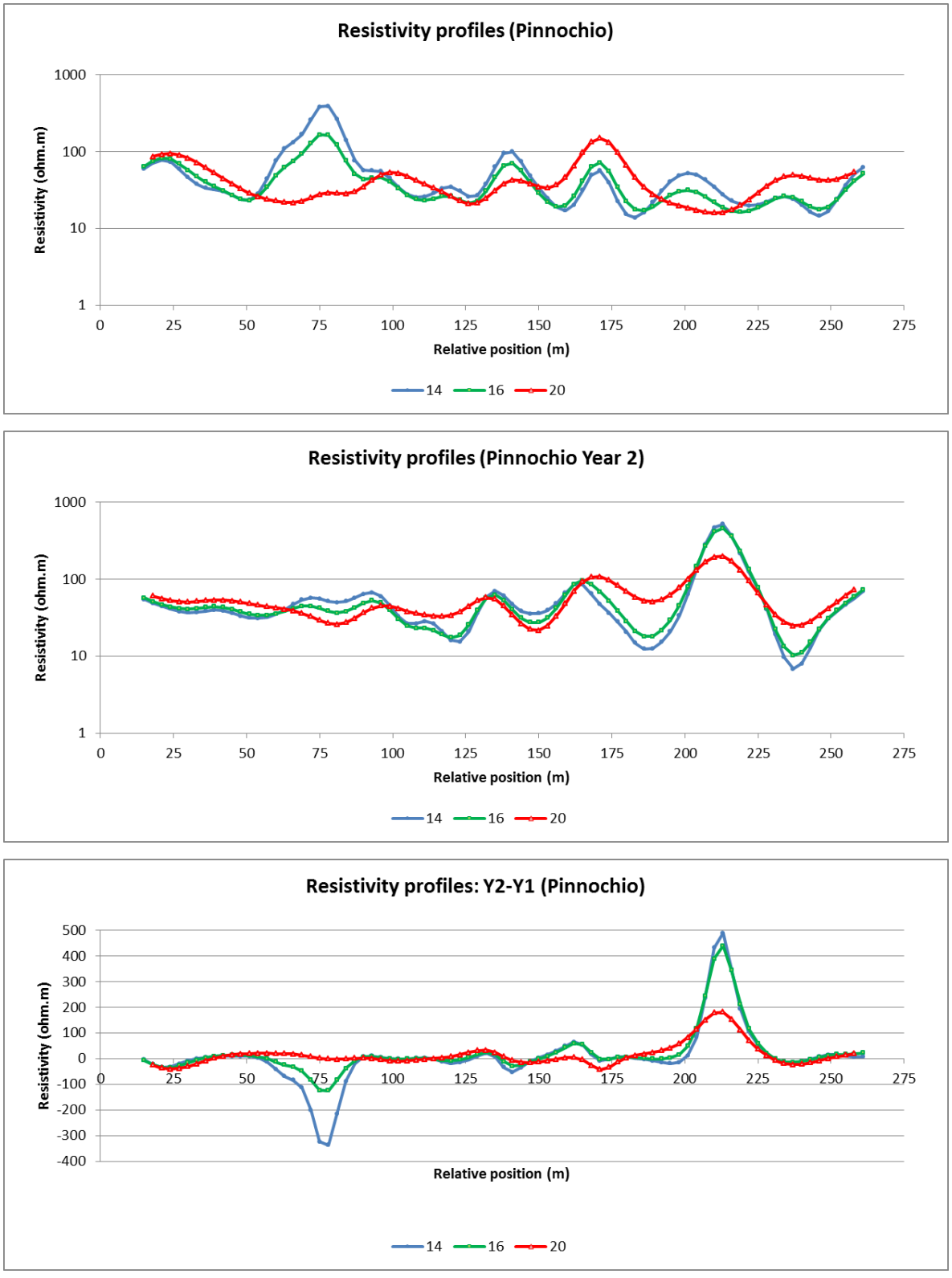

Figure 31: Selected resistivity-depth profiles for Pinocchio's Farm and comparison with Year 1 equivalents

5.3 Crisuel Farm Repeat Survey

The Crisuel Farm repeat survey was conducted on 19 June 2017, 495 days or just over 16 months after the baseline survey. As before, care was taken to relocate the electrode positions with as much accuracy as possible and to use the same measurement scheme as in Year 1. The comparative inversion results are shown in Figure 32, while comparative resistivity-depth profiles are presented in Figure 33.

The Year 2 ERT image is relatively similar to the Year 1 output (Figure 32). The highest conductivities (in the near-surface and at depth) are again observed closest to the stream close to electrode #1. The Year 2 output does reveal a definite increase in the very-near-surface resistivity compared to Year 1. This can be attributed to the much drier soil conditions and higher contact resistances experienced during the follow-up survey. The deeper, central depth zone of the area appears to be associated with a lesser degree of change over time; this is also evident in the comparisons of the resistivity-depth difference plots in Figure 33. The only area along the spread where the resistivity changes over time appear more intense and extend significantly deeper, lies approximately between electrodes #10 and #17. This zone is most likely associated with the inferred paleo sinkhole structure referred to in the Year 1 discussion of results; the apparent drastic increase in resistivity could be attributed to the paleo sinkhole structure drying out.

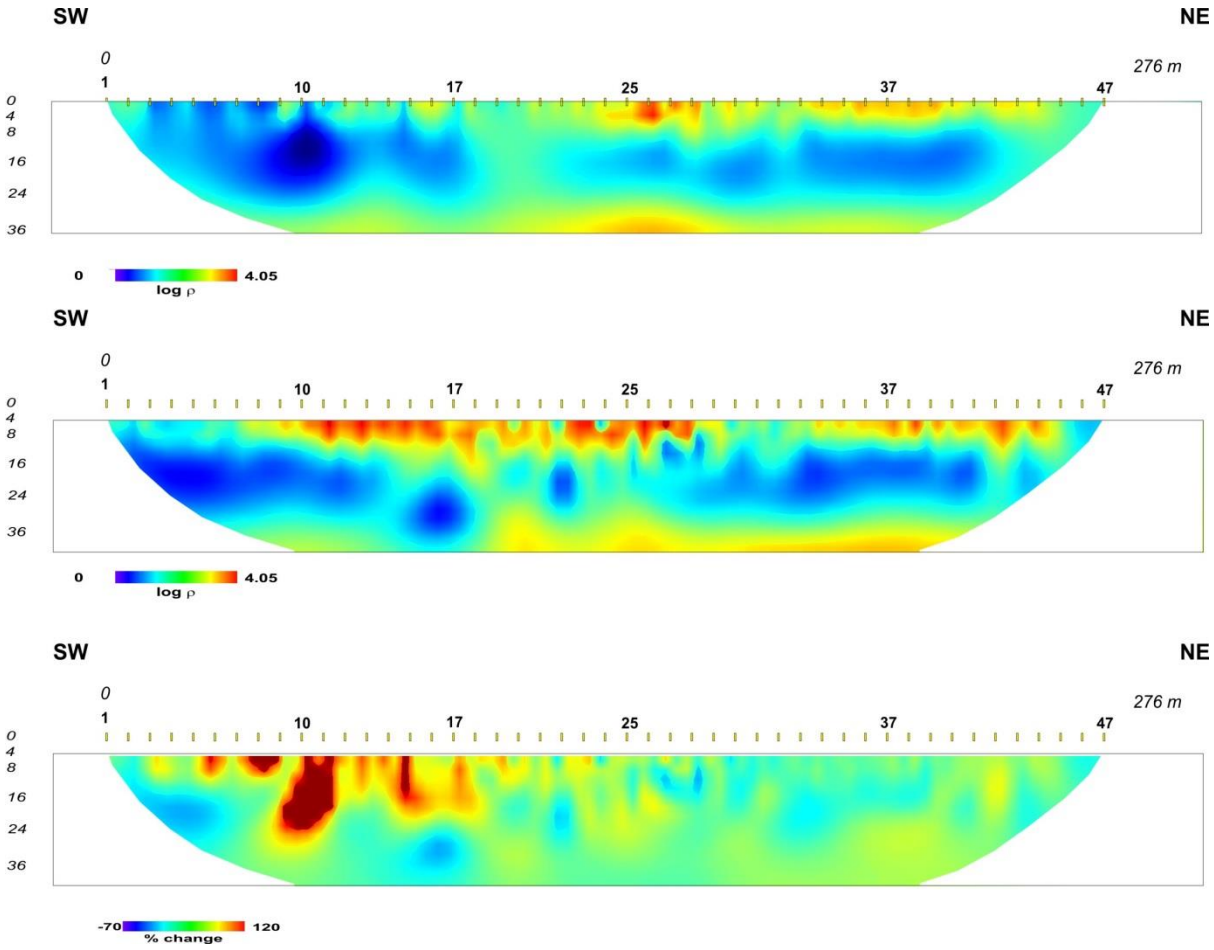

Figure 32: Results of 2017 repeat survey at Crisuel Farm and comparison with Year 1 result

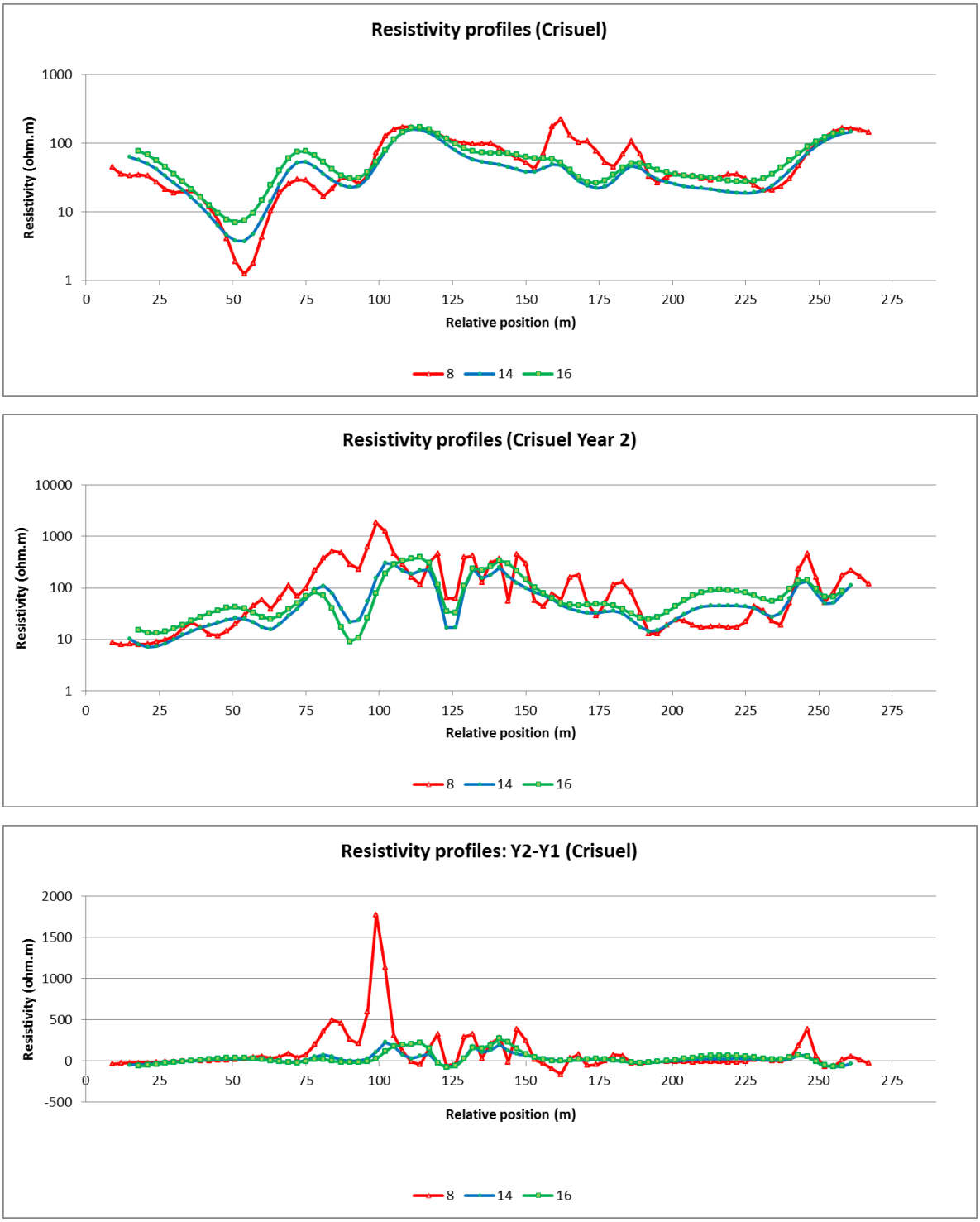

Figure 33: Selected resistivity-depth profiles for Crisuel Farm and comparison with Year 1 equivalents

As was the case at Pinocchio's Farm, an attempt was made to correlate the ERT results with available borehole information. At Crisuel, borehole GP00312, located right next to the ERT profile, was used for this purpose. In December 2015, the sulphate level in GP00312 was 1770 mg/L and the corresponding electrical conductivity value was ~225 mS/m. By July 2016, these values appeared virtually unchanged at 1790 mg/L and 280 mS/m, respectively. By February 2017, shortly before the ERT repeat survey, it had decreased significantly to 1480 mg/L (electrical conductivity = 245 mS/m). This change in sulphate level over the last year equates to approximately 17%. If one ignored the relatively erratic first part of the resistivity responses in Figure 33, and only focussed on the portion of the profiles between approximately x = 150 and the borehole location (x ~250 m), it is possible to identify a marginally

positive resistivity difference, especially for the two deeper difference profiles. However, as was the case at Pinocchio's Farm, the correlation between the sampled sulphate levels and the ERT resistivity responses is complicated because the change in groundwater sulphate level probably does not equate to a clearly detectable change in the bulk aquifer resistivity response. Also, the resistivity variations within the aquifer further complicates such correlation efforts.

5.4 KGR Repeat Survey

The KGR repeat survey was conducted on 20 June 2017, 476 days or approximately 15 months after the original survey. As before, care was taken to relocate the electrode positions with as much accuracy as possible and to use the same measurement scheme as in 2016. Unfortunately, a discrepancy was discovered in this regard during the processing stage. It was realised that the original KGR survey was done using a 7 m unit electrode spacing and not 6 m, as was the case with all other Year 1 surveys. The processing of the KGR data set done in Year 1 also (incorrectly) assumed the 6 m spacing and, consequently, the data acquisition during the repeat survey in 2017, thus inadvertently used the 6 m spacing reflected in the processed results as the correct field parameter. The result is that Year 1 data had to be reprocessed using the correct parameterisation (reflecting the actual 7 m unit electrode spacing used), while the Year 2 data was processed using a 6 m unit electrode spacing. Consequently, the two images in Figure 34 do not have the same horizontal scaling. This discrepancy has complicated the analysis in which changes between these two snapshot images are of interest. Qualitatively, the two ERT images (and associated resistivity-depth profiles in Figure 35) show very similar trends, but a more in-depth, quantitative analysis in the form of Y2-Y1 (difference) plots is not possible.

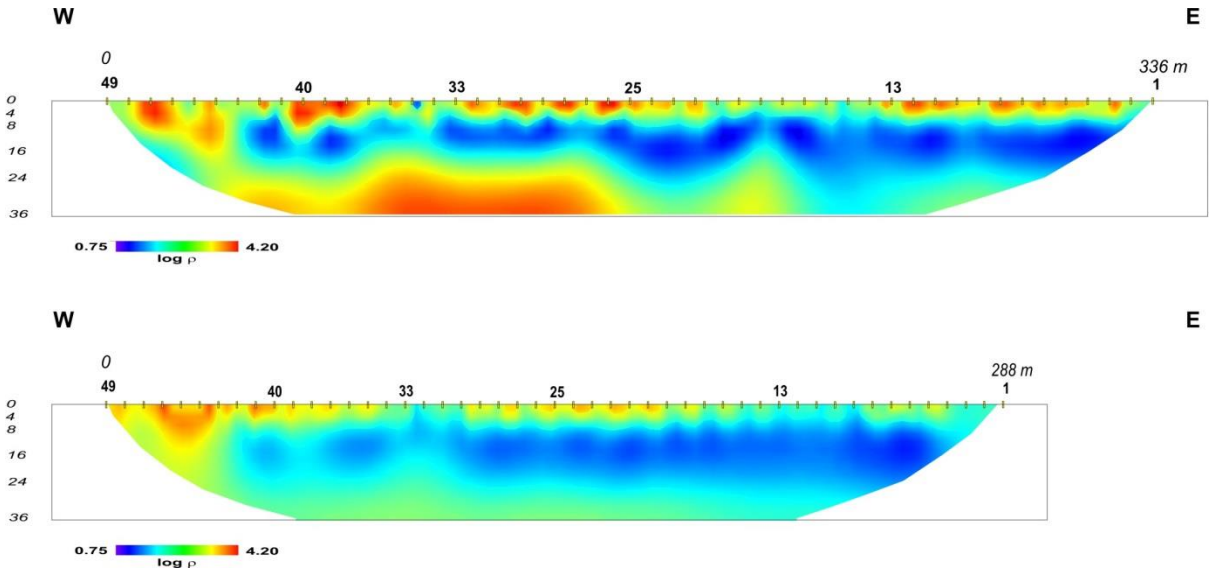

Figure 34: Results of the 2017 KGR repeat survey and comparison with Year 1 result

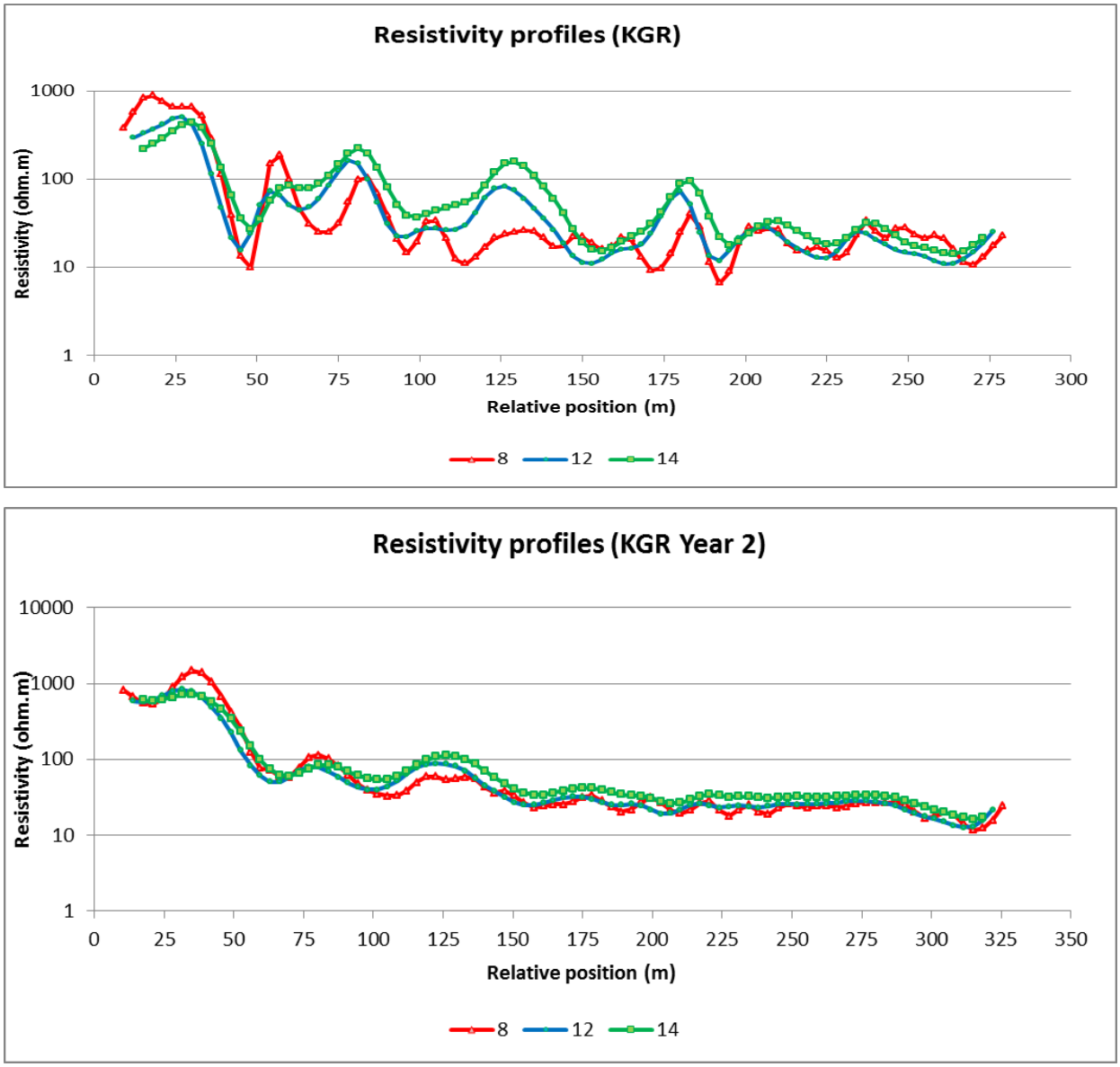

Figure 35: Selected resistivity-depth profiles for KGR and comparison with Year 1 equivalents

5.5 Olwazini Repeat Survey

The Olwazini repeat survey was conducted on 21 June 2017, 448 days or approximately 14.5 months after the original survey. As before, the Year 1 electrode positions were revisited as accurately as possible and the same measurement scheme was also used.

The inversion results for Year 1 and Year 2 are compared in Figure 36. Selected resistivity-depth profiles are compared in Figure 37.

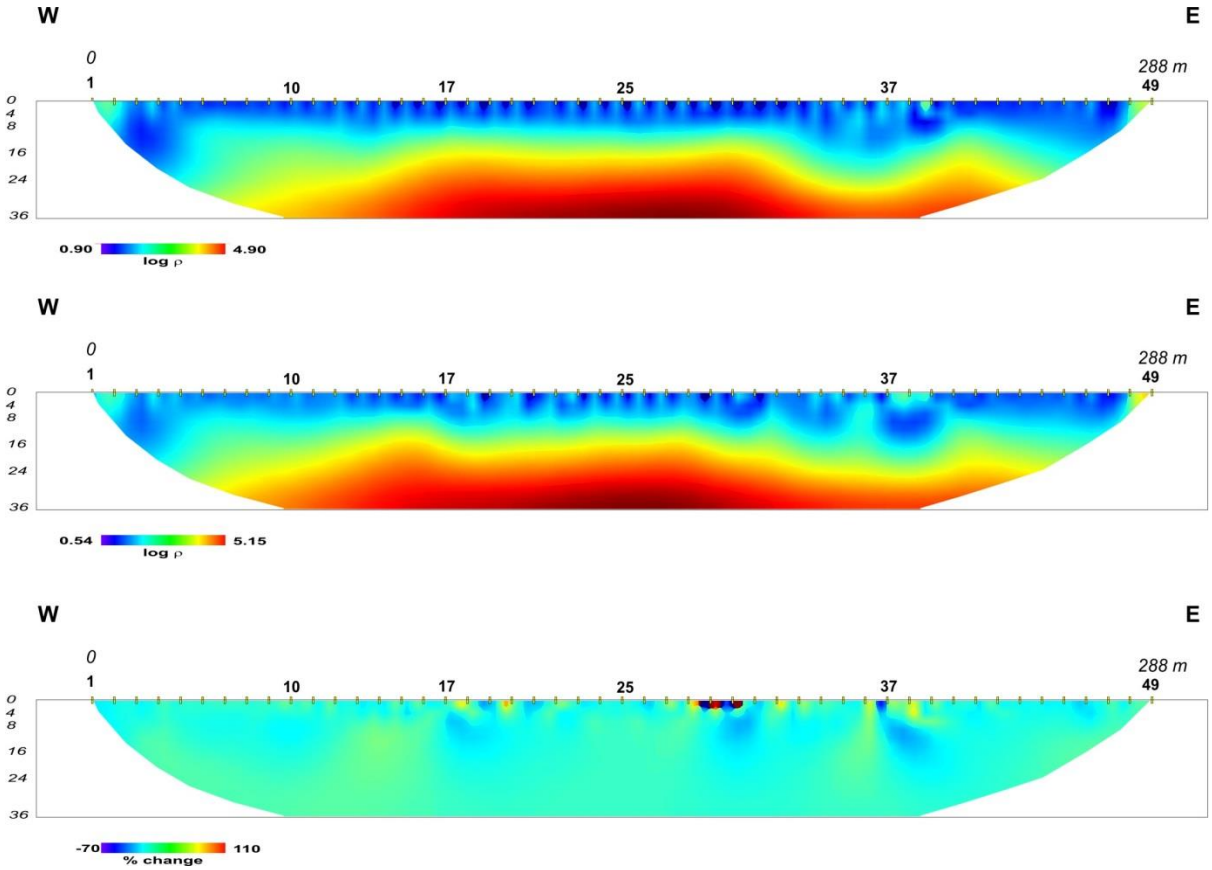

Figure 36: Results of 2017 repeat survey at Olwazini and comparison with Year 1 result

Of all the test sites, the Olwazini repeat survey shows the most striking resemblance with the baseline survey results. This is evident in both the tomographic reconstructions and the selected resistivity-depth profiles. There appears to be only two locations where reasonably significant changes from Year 1 to Year 2 can be observed – around x = 75 m and around x = 175 m (see difference plots in Figure 37). It is interesting to note that these changes appear not to be associated with very near-surface changes, but rather with deeper changes as these transient anomalies are more prominent on the 12 m and 14 m depth difference plots compared to the shallower 8 m difference plot. It was not possible to ascertain the cause of these anomalies. It should, however, be noted that these localised anomalies are not of as much interest in this study as the average background change in the upper portion of the aquifer. It can be seen from the Y2–Y1 plot in Figure 37 that the level of change (localised anomalies apart) is around zero, as suggested by the tomographic images.

As was the case at some of the other test sites, it was unfortunately not possible to do a quantitative comparison between the geophysical results and local borehole results due to the absence of a sampling/test borehole at the site. This is another lesson learnt from this study – in experimental studies proper ground-truthing plays an important part in evaluating test survey results. More care should be taken during test site selection in future similar studies. Alternatively, the sampling and analysis of local aquifer properties should ideally be planned and budgeted for in these type of research project.

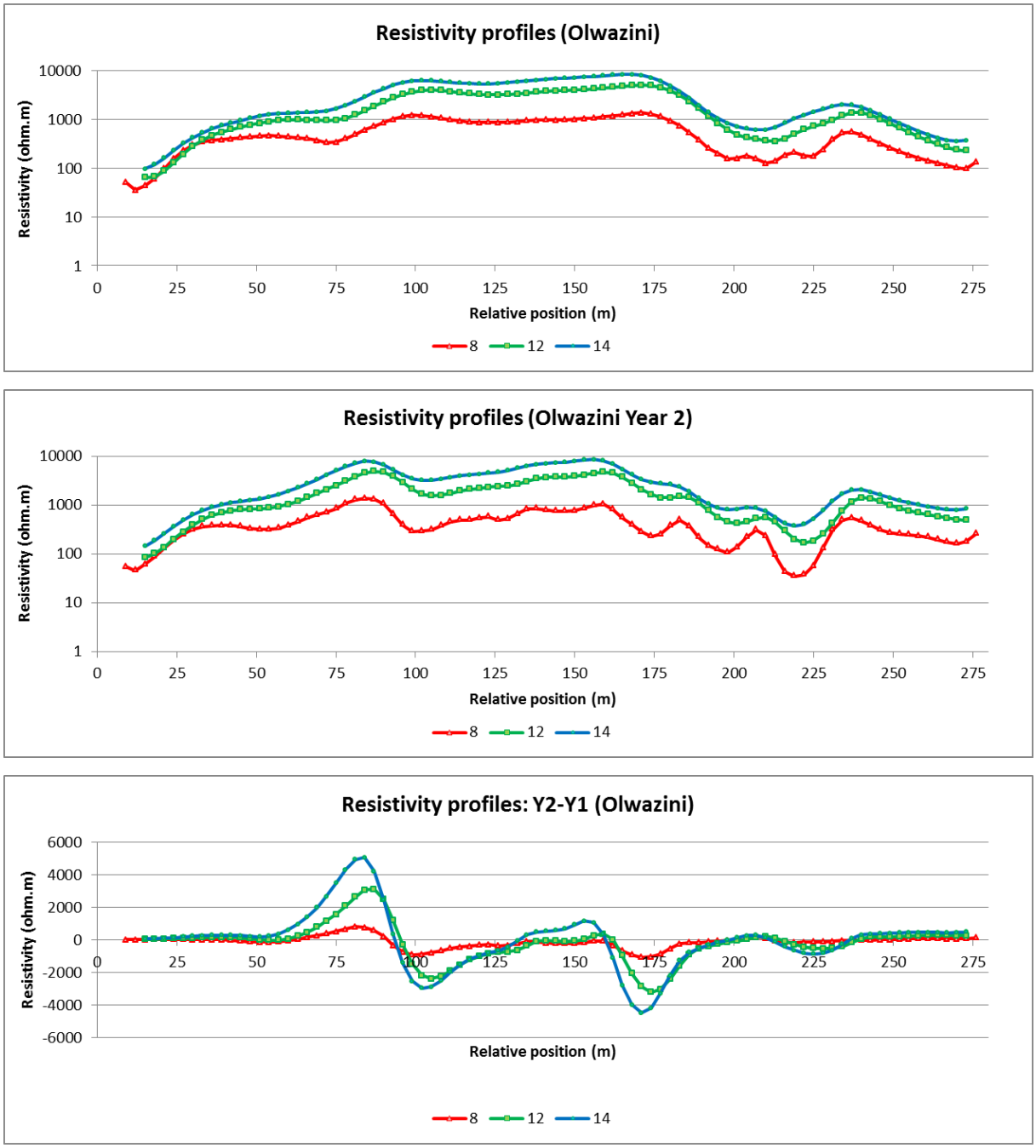

Figure 37: Selected resistivity-depth profiles for Olwazini and comparison with Year 1 equivalents

6 CONCLUSIONS AND RECOMMENDATIONS

The aim of this two-year research project was to demonstrate and advocate using a time-lapse ERT survey method for monitoring the changes in pollution levels (specifically sulphate level) of the local contaminated karst aquifer. To this end, five test sites were selected at the start of the project where such experimental surveys were to be conducted. These surveys involved a baseline survey in Year 1 and a repeat survey in Year 2 at each of the respective sites.

The underlying idea of a time-lapse ERT approach is based on the fact that electrical resistivity is not only a function of a single parameter such as salinity, but is rather a function of a variety of factors such as clay content, mineralogy and pore space characteristics. This implies that a single snapshot ERT survey cannot be used to derive quantitative information relating to only a single parameter. However, by applying a time-lapse or ‘difference tomography’ survey approach, this obstacle can be overcome:

By comparing the results of two tomographic images taken approximately a year apart – and only highlighting the relative change – one could in principle suppress the contribution of those parameters that change slowly over time (or not at all), while emphasising those that do change in the short term. In the case of the AMD-affected COH karst aquifers, the only likely short-term changes in subsurface resistivity can therefore be attributed to changes in the sulphate levels.

An attempt was made to select sites that represent a range of different pollution scenarios. Three of these sites represented relatively high-contamination scenarios (Crisuel and KGR), one could be considered to be moderately contaminated (Pinocchio), one had relatively low sulphate levels (Boland), while the final site (Olwazini) was chosen as a control site as it was expected to have virtually no sulphate contamination and thus also a low likelihood of significant short-term transient changes in the associated subsurface resistivity structure.

Two independent numerical model studies were employed during the course of the project to support some of the decisions and inferences made. At the start of the project, a series of computer simulations were used to justify the decision to employ the multi-gradient electrode array and associate measurement scheme instead of other more commonly used arrays such as the dipole-dipole and Wenner arrays. One of the reasons for this choice was a better signal-to-noise ability, as it was initially anticipated that induced polarisation data would also be used in the study. However, the induced polarisation data quality was generally not high enough to enable meaningful tomographic reconstructions and were therefore not included in the analyses.

A second model study, which was conducted in Year 2 by a student (S'bonelo Zulu) on the project, was aimed at assessing and benchmarking the applicability of the proposed time-lapse ERT approach. In short, this study, which also helped S'bonelo earn his MSc in Geohydrology (University of the Witwatersrand), confirmed that it was possible to use time-lapse ERT to detect subtle changes in near-surface aquifer resistivity. His study also highlighted that the effectiveness of the time-lapse approach will be compromised in cases where the area affected by change is relative small (localised) or relatively deep. The ability to detect resistivity changes is also smaller for small effective contrasts (ratio between the resistivity of the target zone before and after the change).

In practice, the gross resistivity structures observed in the baseline surveys at each test site were again observed in the repeat surveys. However, some localised anomalous changes – in some cases relatively significant – were observed and it was not clear in all cases whether these changes were related to artefacts (for example, due to electrode relocation inaccuracies) or to actual changes in the subsurface properties (for example, due to drier soil conditions experienced in the Crisuel repeat survey).

In one instance (Boland Farm), a complete quality control and reprocessing of the Year 1 and Year 2 data sets were conducted as the discrepancies between the baseline and repeat survey outputs were difficult to explain in terms of short-term near-surface transient changes. The possibility was investigated that an inadvertent processing error or non-random (systematic) error could have caused the observed discrepancies. After the reprocessing efforts, some discrepancies still remained and systematic error was the only reasonable explanation (possible malfunctioning electrode take-out cables suspected during Year 1 survey).

For the cases where the data enabled a meaningful time-lapse analysis, it was found that the observed changes in the background aquifer resistivity were very small (near-zero). It is inferred that the actual changes in aquifer resistivity over the period between the Year 1 and Year 2 were likely too subtle to manifest as prominent anomalies on the difference images. There were, however, some promising indications, particularly at Crisuel Farm, that transient changes in aquifer sulphate levels could possibly be detected using time-lapse ERT measurements.

Although the overall results in this research project do not serve to clearly justify the routine use of the time-lapse ERT method in the COH area, there were sufficient promising indications and lessons learnt to suggest that the approach is a reasonable option in terms of providing supplementary information for

traditional borehole sampling approaches. Should any future time-lapse ERT studies be commissioned, the following recommendations should be considered:

- To eliminate relocation errors, it is strongly advised to employ permanent electrodes. The electrodes may be in the form of conductive electrodes buried or grouted into the shallow subsurface. It is appreciated that this may be logistically challenging and not possible in all places, but the initial effort will be worth the gain in increased data reliability.
- Test site selection should be done more stringently to select sites that are close to, or perhaps between, existing monitoring boreholes. This will enable better correlation with geohydrological parameters and will supplement the borehole information by adding data between the points associated with the borehole locations.
- Test site selection could perhaps also be improved by doing a number of reconnaissance profiles in an area of interest. This will enable the identification of geological features that one needs to either focus on or would want to avoid for the purpose of monitoring.
- ERT data acquisition can be speeded up significantly and automated by using a fully automatic multi-channel receiver system. Such a system will also enable better noise suppression and noise characterisation through the use of increased stacking/averaging, the acquisition of larger data sets and the acquisition of reciprocal measurements.
- In this project, an attempt was made to detect changes over a relatively short period of 12–15 months using a single repeat survey. Ideally, one needs to monitor more frequently and over long periods of time to increase the chances of observing changes in subsurface resistivity and better characterise these transient changes.
- It is also advised to take seasonal effects into consideration when planning surveys and analysing results. For example, comparing surveys done shortly after a period of heavy rainfall with surveys done during the drier months may produce misleading results as significant resistivity changes in the shallow near-surface may dominate over or even distort deeper resistivity anomalies associated with the karst aquifer of interest.
- Finally, this project focussed on using a ground-based geophysical method employing near-DC source fields. The applicability of other techniques that also evaluate subsurface conductivity such as ground- and airborne electromagnetics could also be considered in future studies of this nature.

REFERENCES

Hobbs, P.J. (2013), Surface water and groundwater resources monitoring, Cradle of Humankind World Heritage Site, Gauteng Province, South Africa: Water resources status report for the period April to September 2013. Report no. CSIR/NRE/WR/ER/2013/0083/A. CSIR. Pretoria. 47 pp.

Kemna, A. (2000), Tomographic inversion of complex resistivity: Theory and application, Ph.D. Thesis, Ruhr University Bochum, Germany.

Van Schoor, M. (2015), Optimisation of 2D ERT and IP tomography surface surveys: Some practical considerations, edited, CSIR.

Zulu, S. (2017), The use of time-lapse electrical resistivity tomography to determine the footprint of acid mine drainage on groundwater, GEOL 7028, Research Report, University of the Witwatersrand.